Evaluation of Bioessential Transition Metal Complexes of β-diketonate derivatives as Promising Anticancer Chemotherapeutics

[1*]Arundhati Gogoi, [2]Pragya Bhusan Sandilya, [3]Kandarpa Kumar Saikia

[1*]Ph. D. Research Scholar, Department of Bioengineering and Technology, GUIST, Gauhati University, Guwahati- 781014, Assam, India. Email: arundhatigogoi389@gmail.com
[2]Ph. D. Research Scholar, Department of Bioengineering and Technology, GUIST, Gauhati University, Guwahati- 781014, Assam India. Email: Pragya.sandilya81@gmail.com
[3]Professor, Department of Bioengineering and Technology, GUIST, Gauhati University, Guwahati-781014, Assam, India. Email: kksaikia@gauhati.ac.in

Abstract
This study explored the antitumor potential of two cobalt(II) β-diketonate complexes: $Co(phen)_2(acac)_2$ (C1) and $Co(dpq)_2(acac)_2$ (C2). Their antiproliferative activities were tested on human cancer cell lines A549 (lung adenocarcinoma), HepG2 (hepatocellular carcinoma), and SK-OV-3 (ovarian carcinoma) using the MTT assay, comparing results to cisplatin as a benchmark. C2 exhibited superior antiproliferative effects, with IC_{50} values between 2.1 to 4.5 μM for cancer cells after 24 hours, while C1 showed values of 3.8 to 10.155 μM, both surpassing cisplatin's IC_{50} of 15.044-67.694 μM. Morphological assessments, including crystal violet and AO/PI staining, alongside DNA laddering and clonogenic assays, confirmed the induction of apoptosis and inhibition of cell proliferation. C2 was minimally toxic to normal Vero cells ($IC_{50} \approx 98$ μM), whereas C1 had moderate toxicity ($IC_{50} \approx 50$ μM), both less than cisplatin (17.523 μM). Flow cytometric analysis revealed that C2 caused S-phase cell cycle arrest. In vivo studies in female Swiss albino mice showed that C2 treatment yielded no significant systemic toxicity in hematological, biochemical, and histopathological evaluations. Overall, C2 demonstrates promising anticancer activity in vitro with high selectivity for cancer cells and favorable in vivo tolerability, suggesting its potential as a safe anticancer candidate with minimal adverse effects.

Keywords: Co(II) metal complexes, cytotoxicity, apoptosis, toxicity profile.

1. Introduction

Cancer remains a leading cause of mortality globally, presenting a daunting public health challenge [1]. The International Agency for Research on Cancer (IARC) reported approximately 20 million new cancer cases and 9.7 million cancer-related deaths in 2022[2]. Lung cancer topped the list of fatal cases, with around 1.82 million deaths (18.7%), followed by colorectal, liver, breast, and stomach cancers. The global cancer incidence is anticipated to increase dramatically, with new cases projected to surpass 35 million annually by 2050. This emphasizes the critical need for improved strategies for cancer prevention, early diagnosis, and treatment[3].

Chemotherapy is a fundamental element of cancer treatment, working alongside surgery, radiotherapy, hormone therapy, and immunotherapy [4]. Despite advances, cancer incidence continues to rise, emphasizing the urgent need for improved, safer chemotherapeutic options[5]. Platinum-based drugs, including cisplatin, are commonly utilized but face challenges such as severe toxicity, drug resistance, and tumor recurrence[6-11]. This has led to increased interest in bioessential transition metal complexes as alternative cancer therapies, particularly cobalt complexes due to their diverse coordination chemistry and selective anticancer properties[12]. Cobalt complexes exert effects by interacting with DNA, enzymes, and cellular signaling pathways, and can induce reactive oxygen species (ROS) that lead to oxidative stress and apoptosis in cancer cells. Furthermore, cobalamin (vitamin B_{12}) is being repurposed to mitigate chemotherapy toxicity and can serve as a targeted drug delivery agent, enhancing uptake by cancer cells. Cobalamin-based conjugates, including those linked to radioisotopes or cytotoxic agents, significantly improve receptor-mediated tumor targeting, thereby enhancing therapeutic efficacy while minimizing off-target effects[13-15]. Overall, cobalt-containing compounds present a promising avenue for the next generation of metal-based anticancer therapeutics.

Cobalt coordination complexes have attracted considerable interest as potential anticancer agents owing to their diverse coordination chemistry and favorable biological properties. In particular, cobalt complexes containing β-diketonate ligands have emerged as promising candidates because β-diketones readily coordinate with metal ions through multiple binding modes, thereby enhancing the physicochemical and pharmacological characteristics of the resulting complexes[16]. Among metal β-diketonate compounds, curcuminoid-based complexes have been the most extensively investigated for their anticancer activity[17-25]. In contrast, β-diketonate complexes of first-row transition metals, including cobalt, manganese, iron, nickel, copper, and zinc, remain relatively underexplored. Consequently, the development and biological evaluation of cobalt β-diketonate complexes may provide valuable insights into the design of novel and effective metal-based anticancer therapeutics [17,26-28].

Based on these findings, the present study evaluated the anticancer potential of two β-diketonatecobalt(II) complexes, C1 and C2 (Figure 1), using a series of in vitro assays. In addition, the in vivo toxicity of the lead compound, C2, was assessed in female Swiss albino mice. The complexes were synthesized and characterized by the research team of the Department of Chemistry, Handique Girls' College, Guwahati, Assam, India.

Building on these findings, the present investigation examined the antiproliferative activity of both complexes against a panel of human cancer cell lines and evaluated the subacute toxicity profile of C2 to assess its safety for further preclinical development.

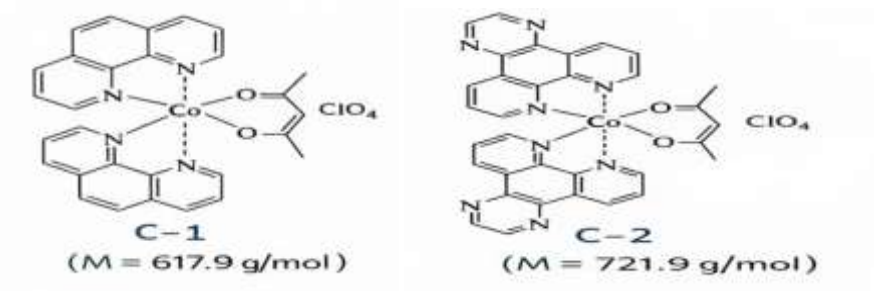

Figure 1: chemical representations of complexes C1 and C2

2. Results and Discussion

2.1 Antiproliferative activity

The Antiproliferative activity of the synthesized β-diketonate Co(II) complexes was evaluated against three human cancer cell lines, A549 (lung adenocarcinoma), HepG2 (hepatocellular carcinoma), and SK-OV-3 (ovarian carcinoma), using the MTT assay[29]. Cells were treated in triplicate with increasing concentrations of the complexes (0.7812–100 μM) for 24 and 48 h, with cisplatin serving as the reference drug. Both Co(II) complexes exhibited significant dose- and time-dependent antiproliferative activity, reducing cell viability across all three cell lines (table 1,Figure 2.1.1-2.3.2). After 24 h of treatment, the complexes showed markedly greater cytotoxicity than cisplatin, with IC_{50} values ranging from 2.1 to 10.15 μM compared with 15.04 to 67.69 μM for cisplatin.

Among the two complexes, C2 exhibited superior cytotoxicity across all three cancer cell lines. After 24 h, C1 showed the greatest activity against HepG2 cells (IC_{50} = 3.87 ± 0.15 μM), followed by A549 cells (4.17 ± 0.05 μM), whereas C2 was most potent against A549 (2.10 ± 0.00 μM) and HepG2 (3.03 μM) cells. Both complexes demonstrated comparatively lower activity against SK-OV-3 cells, although C2 (IC_{50} = 4.58 ± 0.15 μM) remained more potent than C1 (10.16 ± 0.37 μM). Following 48 h of treatment, the cytotoxicity of both complexes further increased, with IC_{50} values ranging from 1.95 to 8.88 μM. C2 exhibited the highest potency against A549 (1.96 ± 0.03 μM), followed by HepG2 (2.26 ± 0.03 μM) and SK-OV-3 (3.65 ± 0.10 μM), while the corresponding IC_{50} values for C1 were 3.75 ± 0.17, 3.34 ± 0.07, and 8.88 ± 0.41 μM, respectively. In contrast, cisplatin showed substantially lower cytotoxicity toward all three cell lines, with IC_{50} values ranging from 9.04 to 37.79 μM.

Table 1. IC50 values (μM) of complexes C1, C2 and cisplatin for 24 h and 48 h treatment, as determined from the MTT assay.

Compound	A549	HepG2	SKOV-3	Vero	SI
C1	4.175± 0.054 3.753±0.171	3.837± 0.154 (3.342±0.067)	10.155±0.372 (8.882±0.411)	50.262±1.103 (55.711±1.175)	13,13,5 14,15,6
C2	2.106±0.083 (1.959±0.026)	3.033±0.179 (2.264±0.031)	4.580± 0.149 (3.645±0.100)	97.55±2.082 (98.759±0.775)	46,32,21 50,44,27
Cisplatin	15.044±0.732 (9.044± 0.23)	24.826±3.302 (8.367±0.412)	67.694±1.505 (37.794±4.351)	17.523±2.569 (10.569±0.088)	2,1, <1 1,1, <1

Values in the parentheses refer to 48 h drug treatment. Selectivity Index (SI) = IC50 (normal cell)/IC50 (cancer cell).

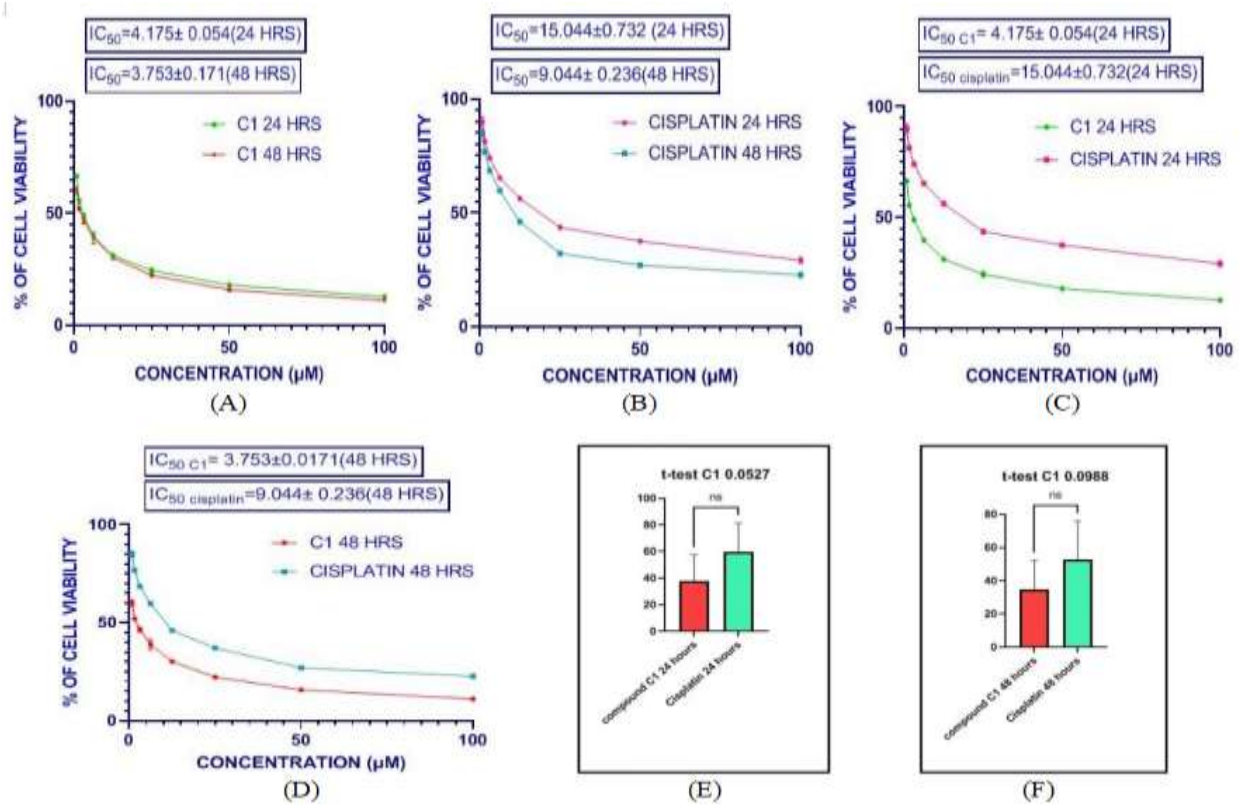

Figure 2.1.1: (A) Graph shows the viability of A549 cells compound C1on in 24 h and 48 h. (B) viability of Cisplatin in 24 and 48 h. (C) viability of compound C1 compared with Cisplatin in 24 h and (D) 48 h. Result of t-test with Cisplatin in 24 h (E) and 48 h (F) showing no significance at the level p <0.05.

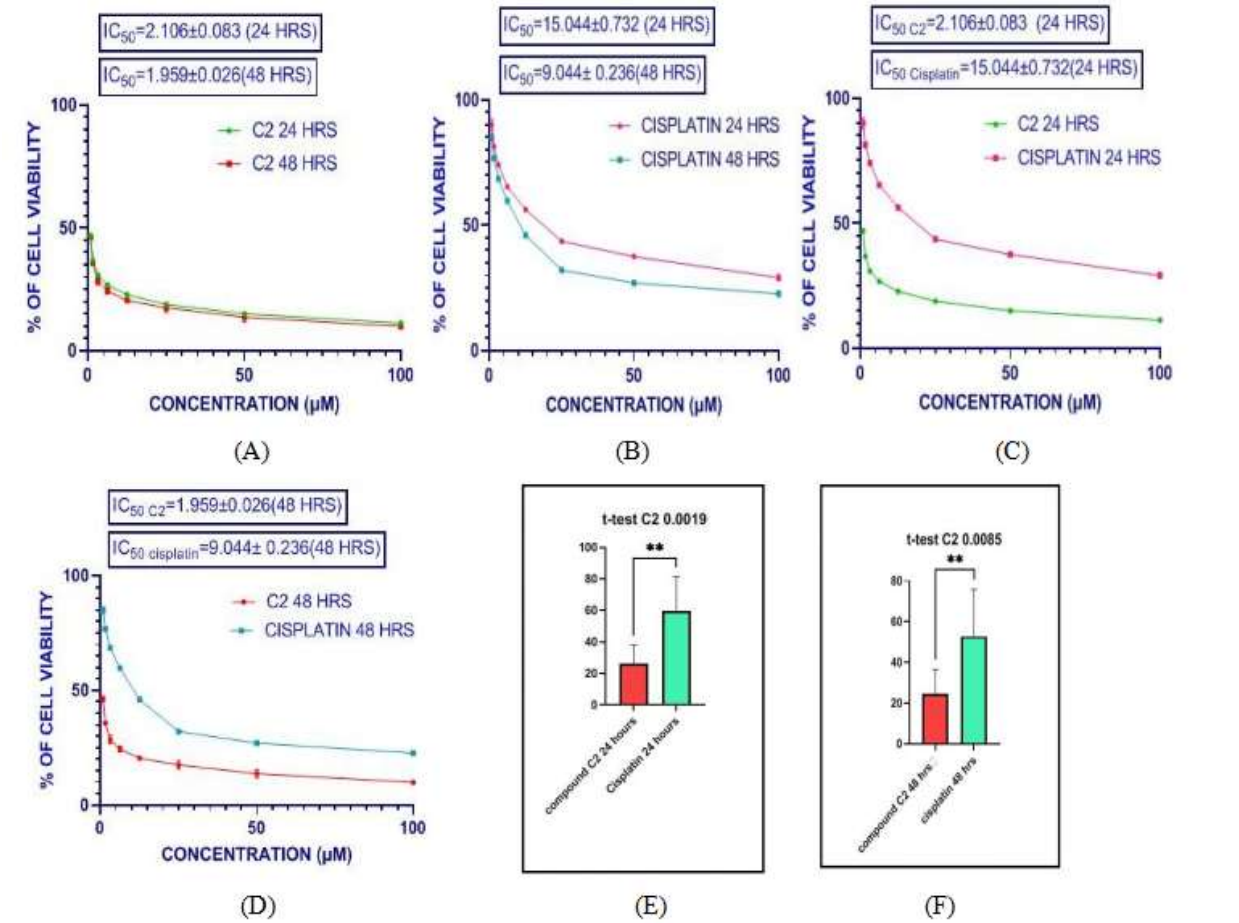

Figure 2.1.2: (A) In vitro viability activity of compound C2 on A549 cell lines in 24 h and 48 h. (B) viability of Cisplatin in 24 and 48 h. (C) viability of compound C2 compared with Cisplatin in 24 h and (D) 48 h. Result of t-test with Cisplatin in 24 h (E) and 48 h (F) showing significance at the level of p<0.01.

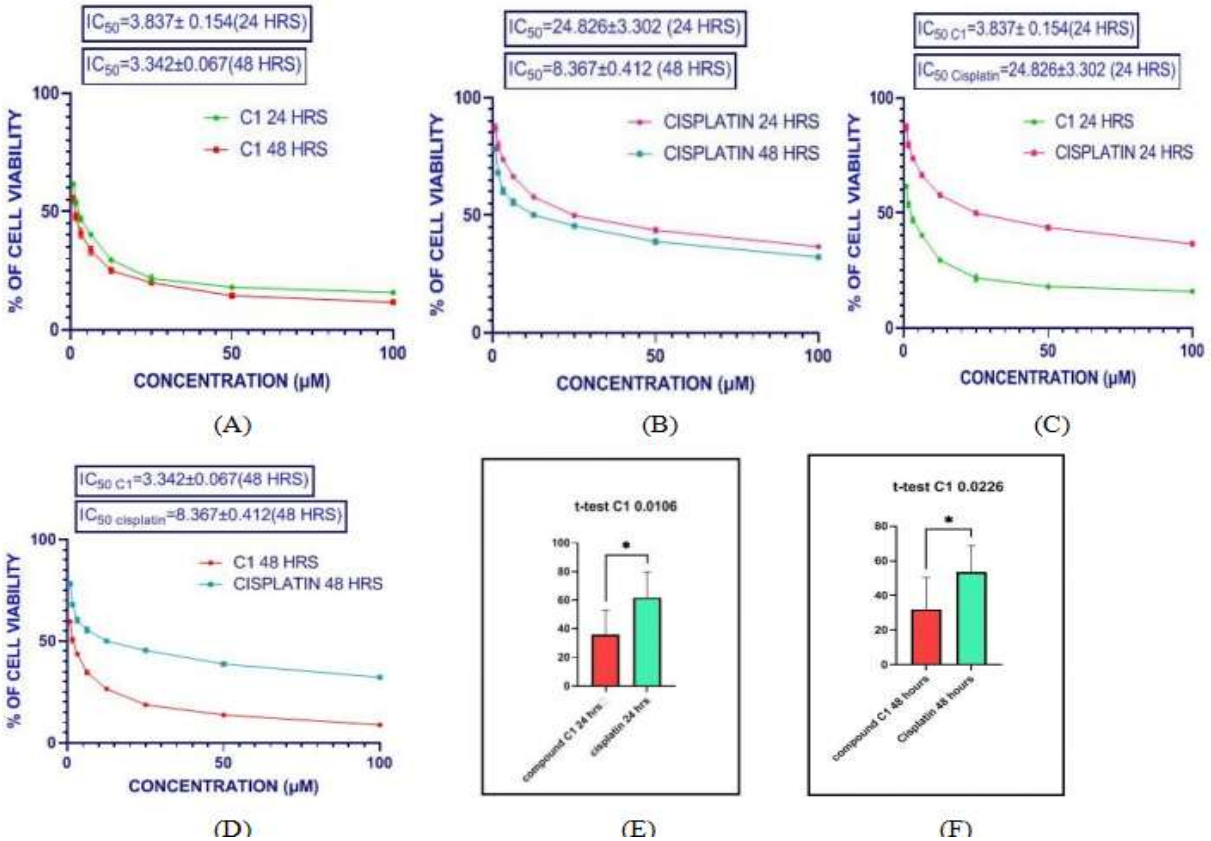

Figure 2.2.1: (A) In vitro viability activity of compound C1on HepG2 cell lines in 24 h and 48 h. (B) viability of Cisplatin in 24 and 48 h. viability of compound C1 compared with Cisplatin in (C) 24h and (D) 48h. Result of t-test with Cisplatin in 24h (E) and 48h (F) showing significance at the level p <0.05.

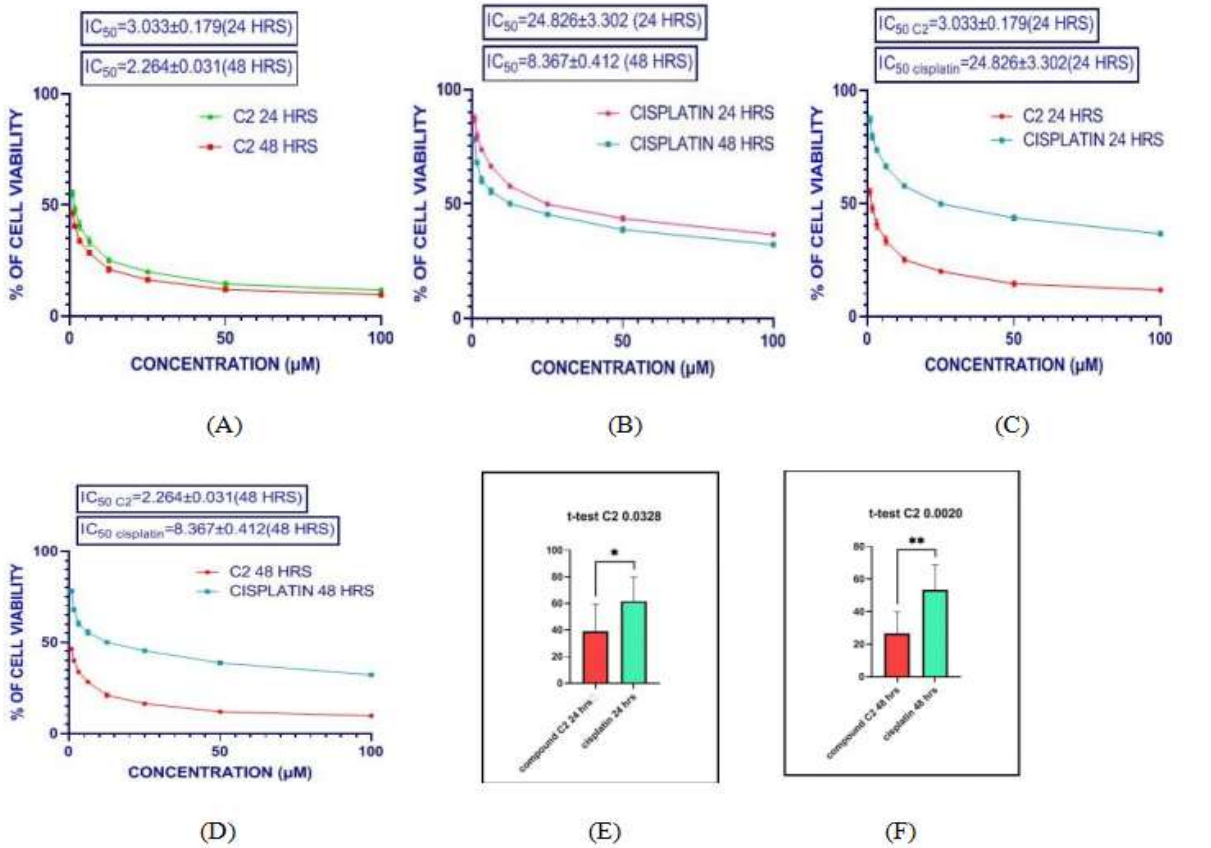

Figure 2.2.2: (A) In vitro viability activity of compound C2 on HepG2 cell lines in 24 h and 48 h. (B) viability of Cisplatin in 24 and 48 h. viability of compound C2 compared with Cisplatin in (C) 24 h and (D) 48 h. Result of t-test with Cisplatin in 24 h (E) and 48 h (F) showing significance at the level of p<0.05 and p<0.01 respectively.

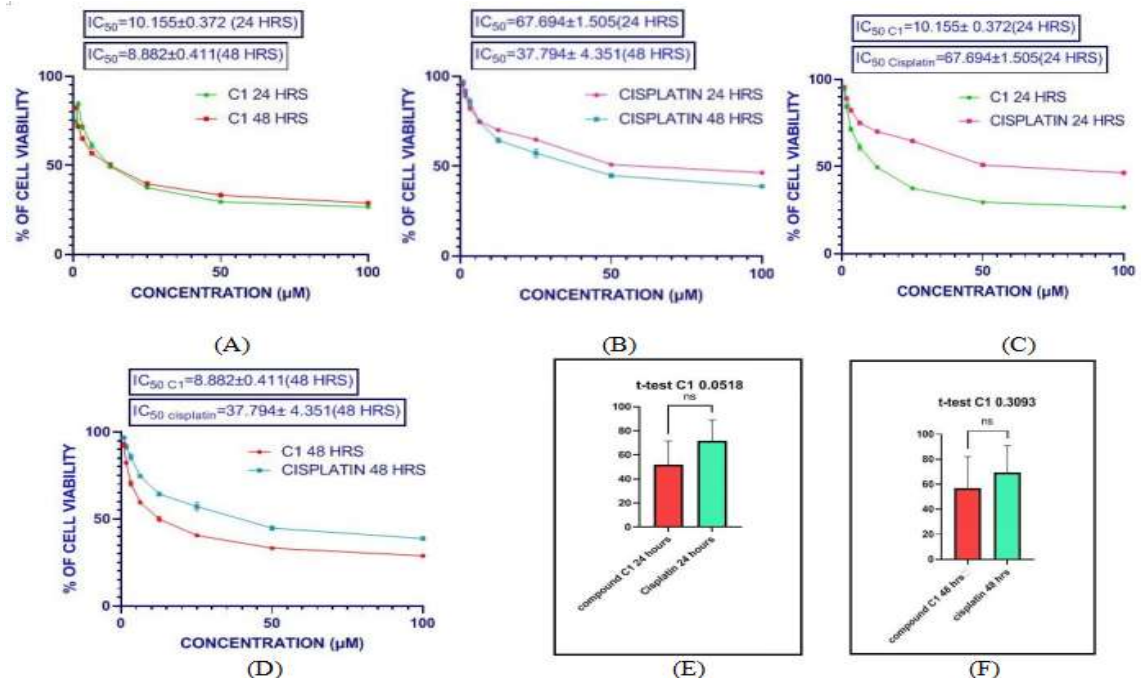

Figure 2.3.1: (A) In vitro viability activity of compound C1 on SKOV3 Cell lines in 24 h and 48 h. (B) viability of Cisplatin in 24 and 48 h. viability of compound C1 compared with Cisplatin in (C) 24 h and (D) 48 h. Result of t-test with Cisplatin in 24 h and 48 h showed no significance with the p value both >0.05.

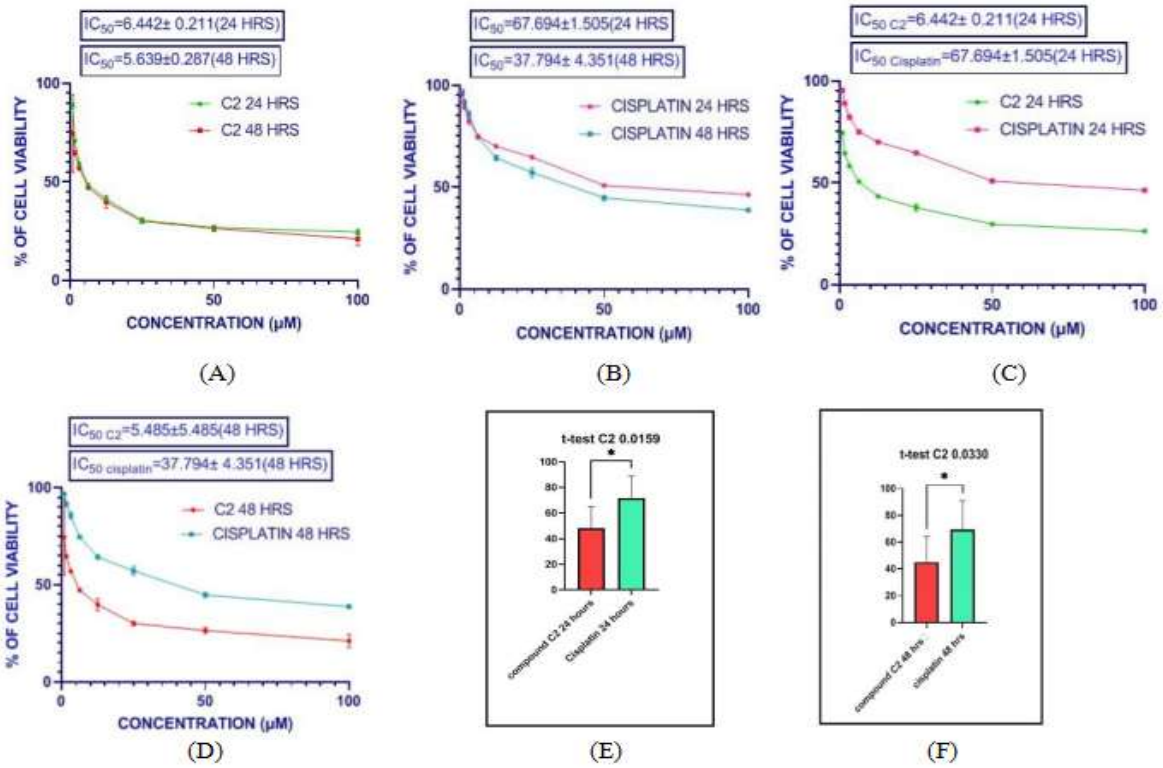

Figure 2.3.2: (A) In vitro viability activity of compound C2 on SKOV3 Cell lines in 24 h and 48 h. (B) viability of Cisplatin in 24 and 48 hrs. viability of compound C2 compared with Cisplatin in (C) 24 hr and (D) 48h Result of t-test with Cisplatin in 24h (E) and 48 h (F) showing significance at the level of p <0.05.

2.2 Cytotoxicity

While exerting its effect on cancer cells, chemotherapeutical agents can produce toxicity on live normal cells which is described as the Cytotoxicity [30]. Cytotoxicity of the tested compounds toward normal cells was evaluated in Vero cells using the MTT assay. Complex C2 exhibited minimal toxicity, with IC_{50} values of 97.55 ± 2.08 µM and 98.76 ± 0.78 µM after 24 and 48 h, respectively. Complex C1 also showed lower toxicity (IC_{50} = 50.26 ± 1.10 µM at 24 h and 55.71 ± 1.18 µM at 48 h) compared to cisplatin, which was markedly cytotoxic to Vero cells (IC_{50} = 17.52 ± 2.57 µM at 24 h and 10.57 ± 0.09 µM at 48 h)(Figures 2.4.1-2.4.2). These findings indicate that both Co(II) complexes, particularly C2, exhibit greater selectivity toward cancer cells than normal cells.

The selectivity index (SI = IC_{50} Vero/IC_{50} cancer cells) was determined to assess the therapeutic selectivity of the Co(II) complexes (Table 1). Both complexes exhibited substantially higher SI values than cisplatin, with selectivity increasing after 48 h of treatment. At 24 h, C1 showed SI values of 13, 13, and 5, whereas C2 exhibited markedly higher SI values of 46, 32, and 21 against A549, HepG2, and SK-OV-3 cells, respectively. After 48 h, the SI values further increased to 14, 15, and 6 for C1 and to 50, 44, and 27 for C2. In contrast, cisplatin displayed SI values below 2 for all cell lines at both time points, consistent with its poor selectivity and known toxicity to normal cells[31-35]. Since SI values >10 indicate high selectivity, C2 demonstrated excellent cancer cell selectivity across all three cell lines, whereas C1 exhibited moderate to high selectivity. These findings identify C2 as the more promising therapeutic candidate.C2 exhibited high selectivity toward all three cancer cell lines, with SI values of 21–46 at 24 h and 27–50 at 48 h. In comparison, C1 showed moderate to high selectivity, with SI values ranging from 5–13 and 6–15 at 24 and 48 h, respectively.

The results indicate that C2 exhibits minimal toxicity toward normal cells and high cancer cell selectivity, whereas C1 showed moderate selectivity. As a higher selectivity index (SI) reflects greater therapeutic safety and efficacy [36], C2 was found suitable for further in vivo toxicity evaluation.

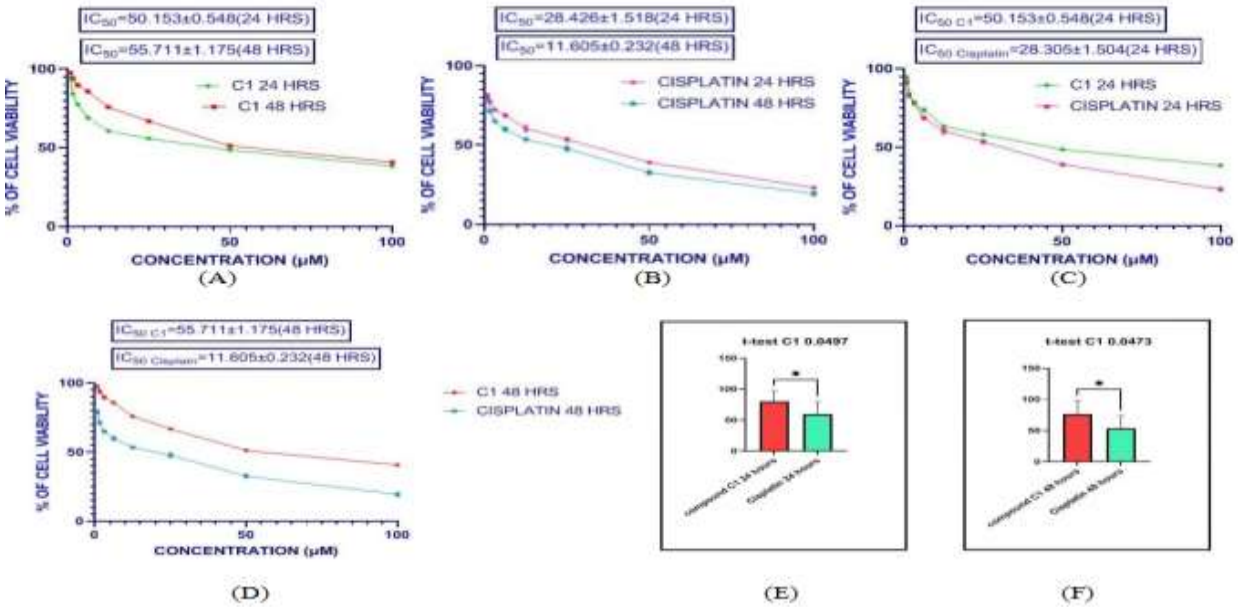

Figure 2.4.1: (A) In vitro viability activity of compound C1 on Vero Cell lines in 24 h and 48 h. (B) viability of Cisplatin in 24 and 48 h. viability of compound C1 compared with Cisplatin in (C) 24 h and (D) 48 h. Result of t-test with Cisplatin in 24 h (E) and 48 h (F) showing significance at the level of p <0.05.

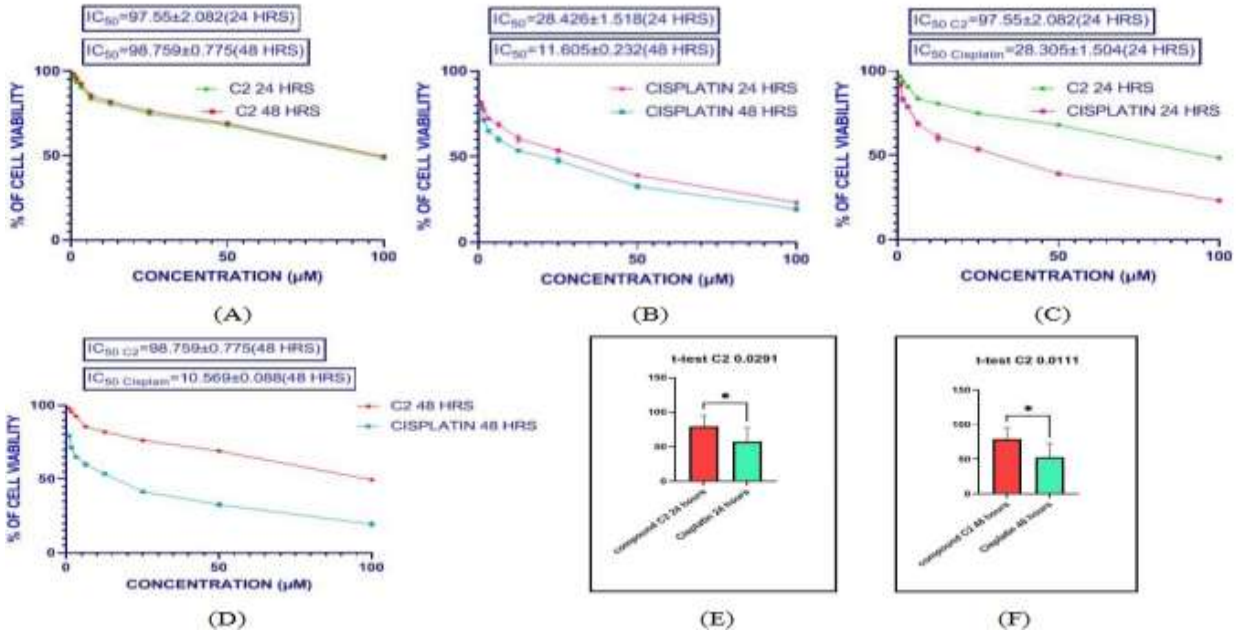

Figure 2.4.2: (A) In vitro viability activity of compound C2 on Vero Cell lines in 24 h and 48 h. (B) viability of Cisplatin in 24h and 48 h. viability of compound C1 compared with Cisplatin in (C) 24 h and (D) 48 h. Result of t-test with Cisplatin in 24 h (E) and 48 h (F) showing significance at the level of p <0.05.

2.3 Cell Morphology Evaluation

Morphological examination revealed dose-dependent cytotoxic effects of the Co(II) complexes, consistent with the MTT assay results (Figures 3.1–3.4) confirming the correlation of morphological- stage-dependent cellular

response[37]. Treated A549, HepG2, and SK-OV-3 cells exhibited characteristic apoptotic features, including cell shrinkage, cytoplasmic condensation, membrane blebbing, apoptotic body formation, and reduced cell density, whereas untreated cells maintained normal morphology. Compared with cisplatin, both Co(II) complexes induced more pronounced morphological changes, indicating enhanced cytotoxicity. Among the two complexes, C2 produced the greatest apoptotic changes at lower concentrations, particularly in A549 cells, followed by HepG2 and SK-OV-3, while C1 showed its strongest effects in HepG2 cells.

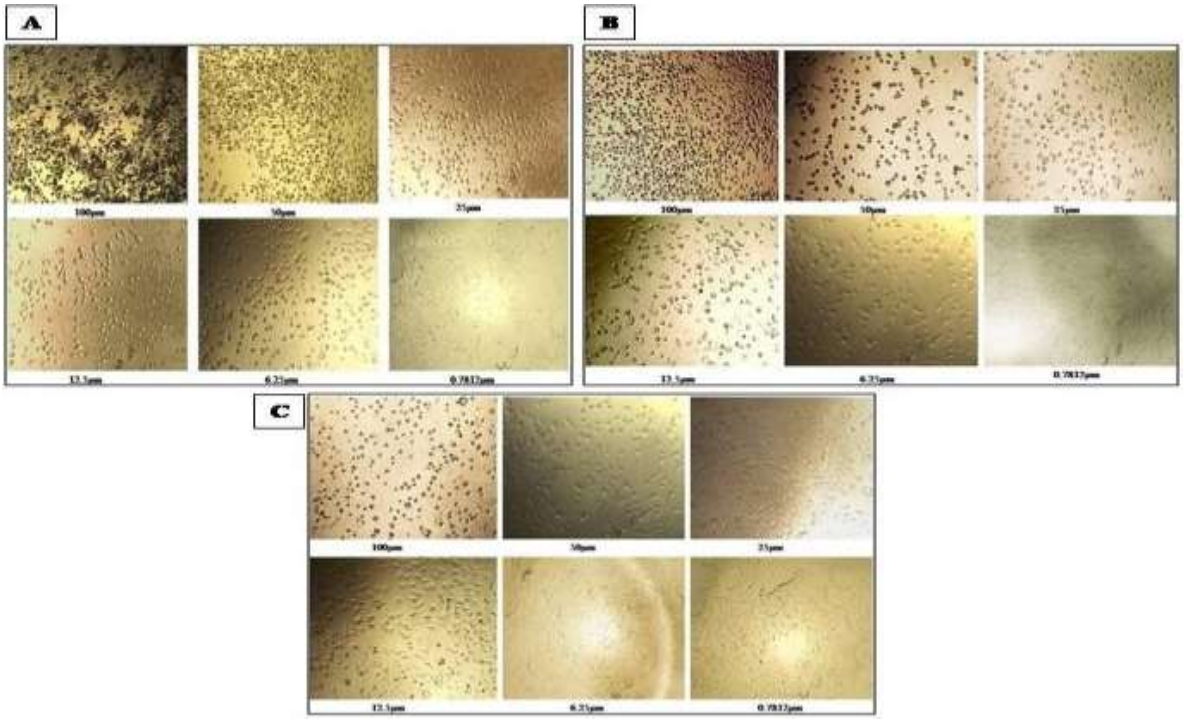

Figure 3.1: Morphological changes of A549 Cells after treatment with different concentrations of (A) compound C1 B) compound C2 and (C) Cisplatin at 24 h.

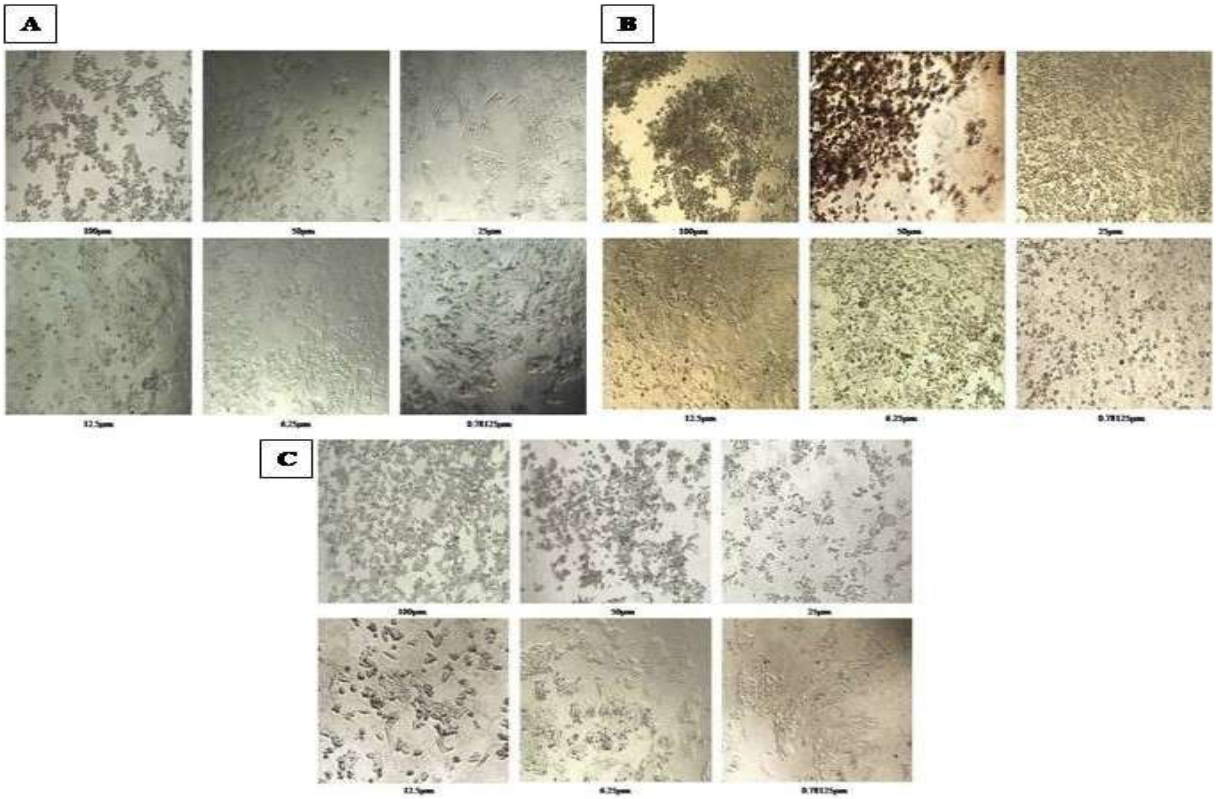

Figure 3.2: Morphological changes of HepG2 Cells after treatment with different concentrations of (A) compound C1 (B) compound C2 and (C) Cisplatin at 24 h.

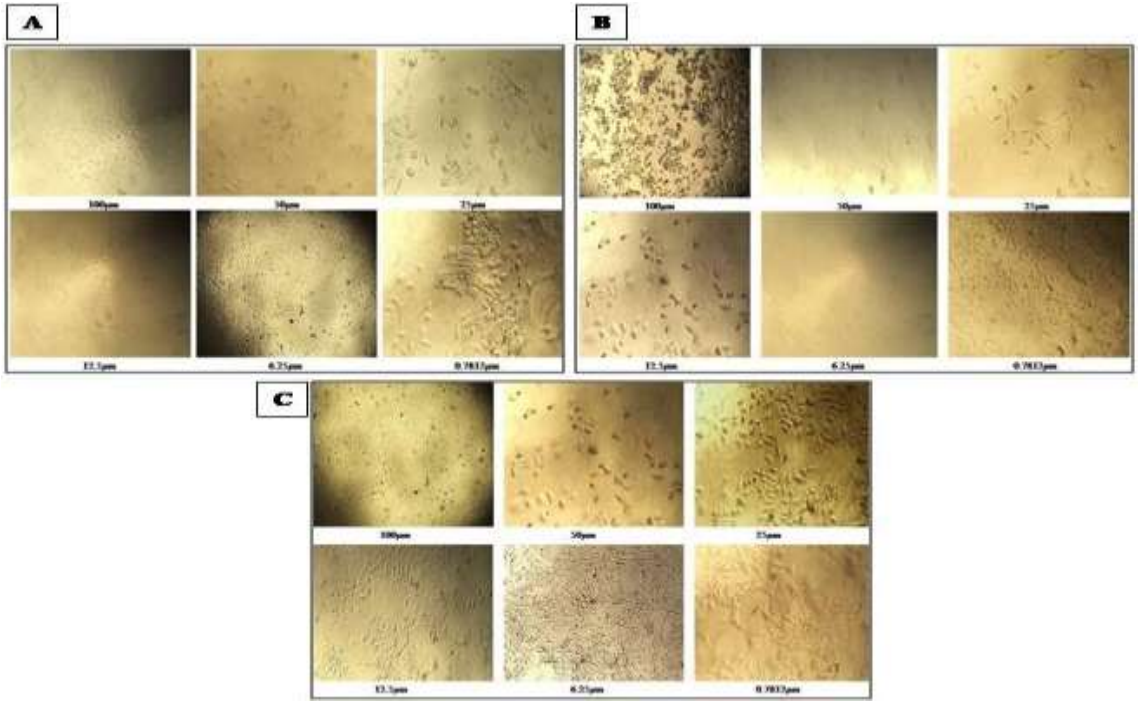

Figure 3.3: Morphological changes of SK-OV-3 Cells after treatment with different concentrations of (A) compound C1 and (B) compound C2 and (C) Cisplatin at 24 h.

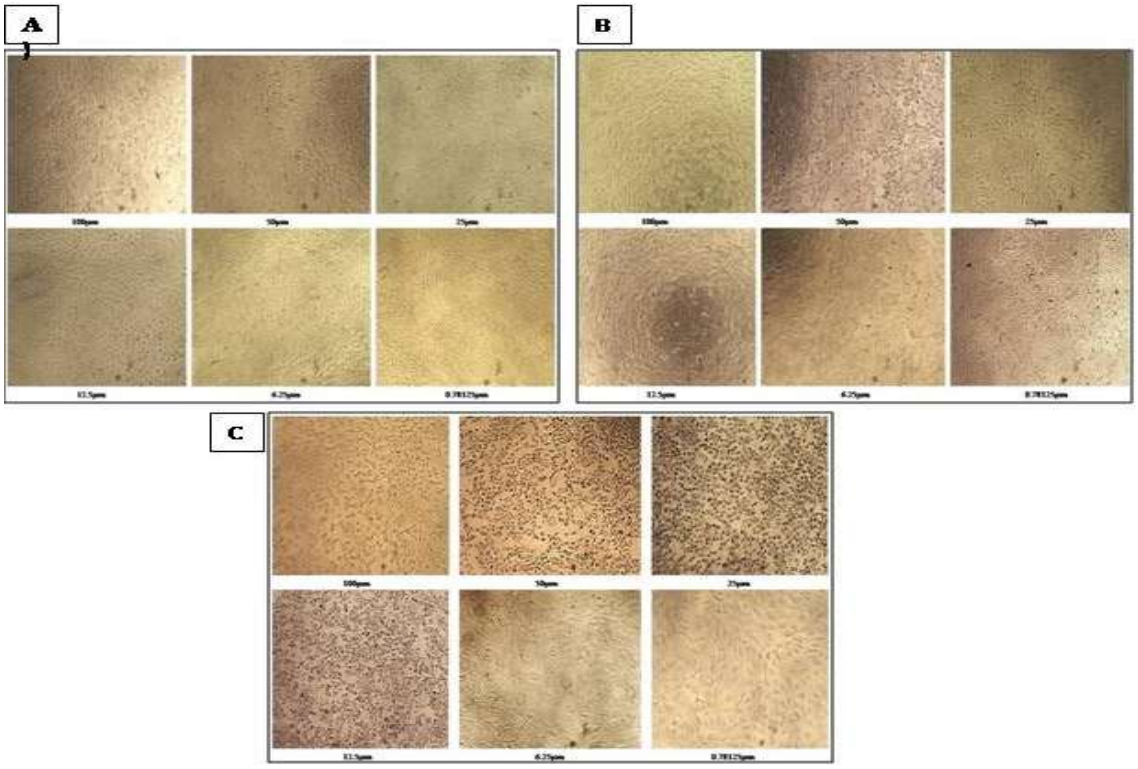

Figure 3.4: Morphological changes of Vero Cells after treatment with different concentrations of (A) compound C1 (B) compound C2 and (C) Cisplatin at 24 h.

2.4 Crystal Violet Staining

The effects of the Co(II) complexes on cell viability and morphology were further evaluated using the crystal violet assay [38,39]. Treatment of A549, HepG2, and SK-OV-3 cells with C1 and C2 at their respective IC_{50} concentrations for 24 h markedly reduced the number of viable cells compared with untreated controls. C2 produced the greatest reduction in crystal violet-stained (viable) cells, followed by C1, whereas cisplatin-treated cells retained comparatively higher viability. These findings confirm the superior cytotoxic activity of the Co(II) complexes, particularly C2, and are consistent with the MTT assay results(Figure.4).

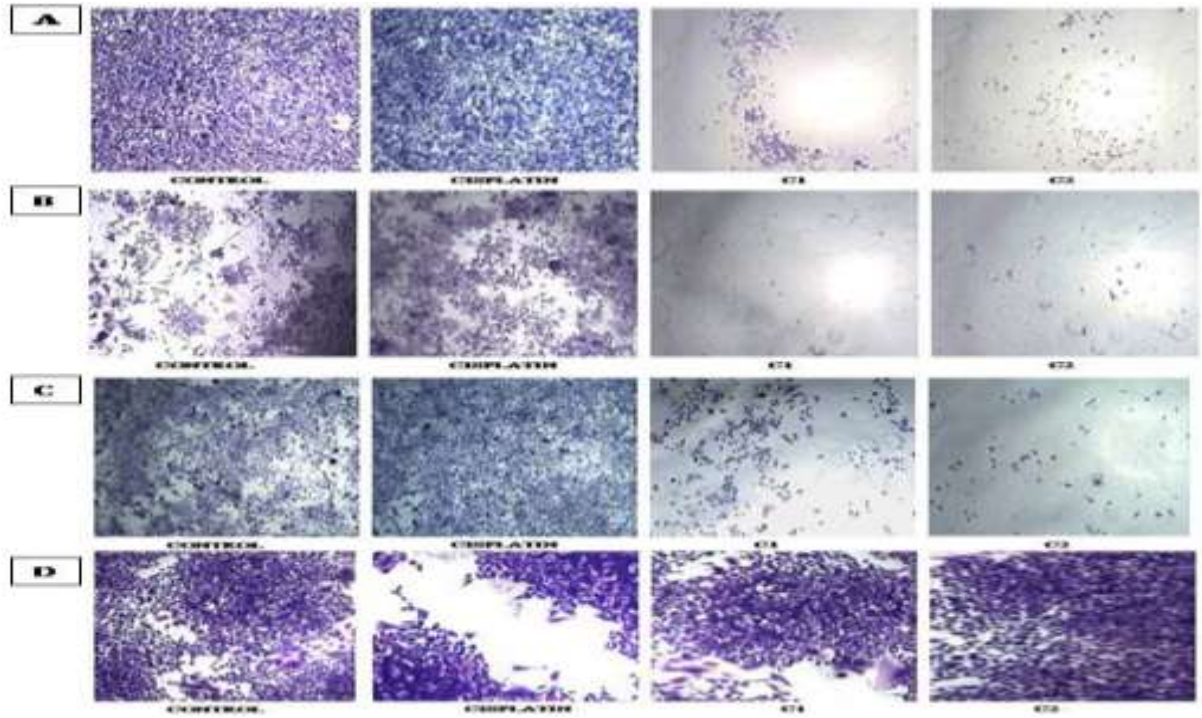

Figure 4: Morphological changes of (A) A549, (B) HepG2, (C) SKOV3 and (D) Vero cells at 4X without any treatment (control), after treatment with the IC50 concentrations of Cisplatin and the test compounds C1 and C2 for 24h.

2.5 AO/PI method

Apoptosis induction by the Co(II) complexes was confirmed using acridine orange/propidium iodide (AO/PI) dual staining, which distinguishes viable, early apoptotic, late apoptotic, and necrotic cells based on differential fluorescence. Differential staining pattern enabled the identification and confirmation of apoptosis induced by the cobalt compounds in the three cancer cell lines [40]. Untreated A549, HepG2, and SK-OV-3 cells exhibited uniform green

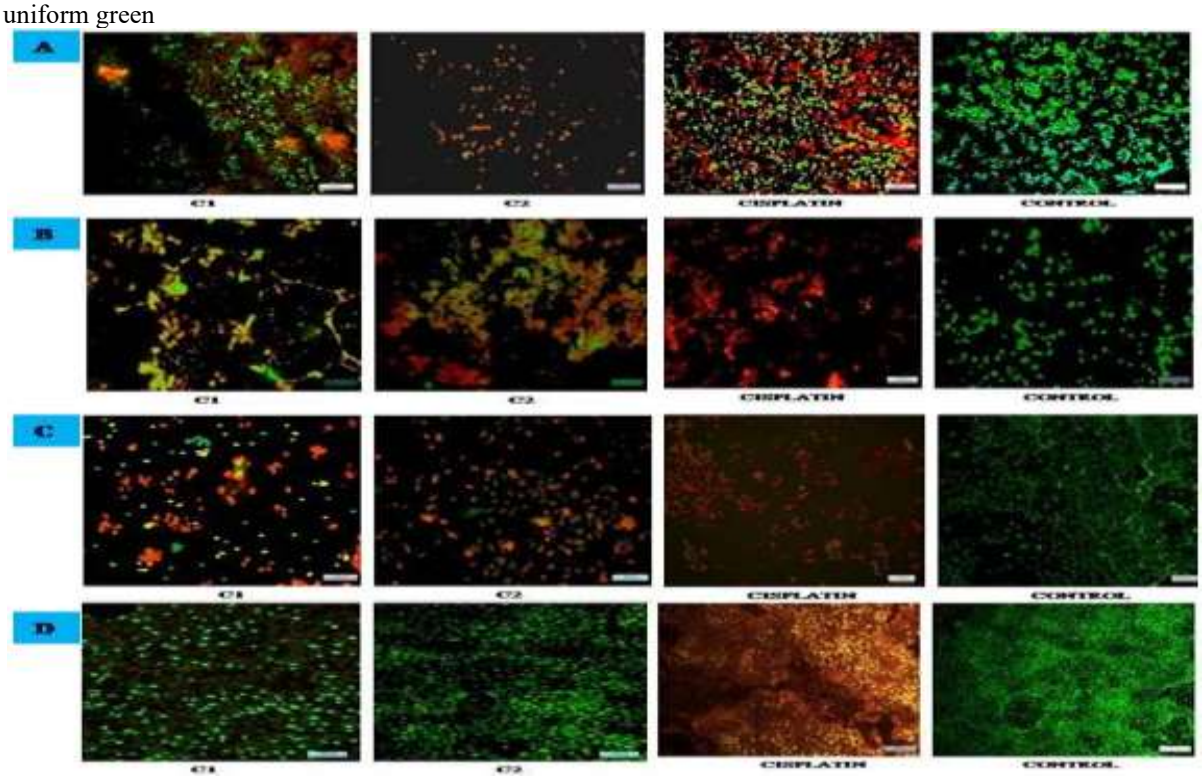

Figure 5.1: Fluorescence microscopy images at 4X of dual AO/PI stained (A) A549, (B) HepG2, (C) SKOV3 and (D) Vero cells after treatment with C1, C2 and Cisplatin and without treatment. The cell lines were treated with an IC_{50} dose of C1, C2 and Cisplatin for 24 hrs. Cells without treatment are taken as Control.

fluorescence, indicating viability, whereas treated cells showed characteristic apoptotic features, including chromatin condensation, membrane blebbing, nuclear fragmentation, cell shrinkage, and apoptotic body formation (Figures 5.1 and 5.2). C1 induced moderate apoptosis, while C2 produced the most pronounced apoptotic morphology with extensive orange/red fluorescence and fewer viable cells, indicating superior pro-apoptotic activity (Figure 5.1). In contrast, cisplatin-treated cells displayed a mixed population of viable,

apoptotic, and necrotic cells. Importantly, C2 caused negligible cytotoxicity in normal Vero cells, which retained fluorescence patterns comparable to untreated controls, whereas cisplatin induced marked apoptosis in Vero cells. These findings demonstrate that C2 selectively induces apoptosis in cancer cells while sparing normal cells.

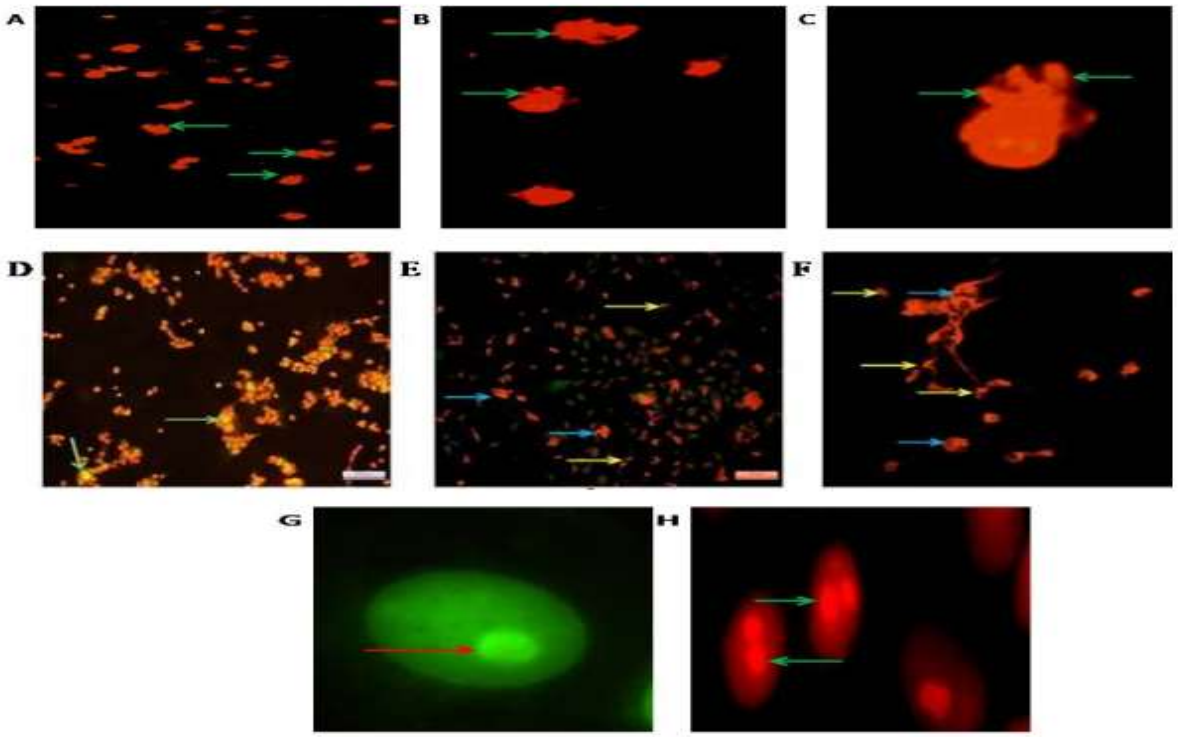

Figure 5.2: Fig (A),(B),(C) Fluorescence microscopy images of membrane blebbing of A549 cells as a sign of Apoptosis and fig (D), (E), (F) Fluorescence microscopy images of different stages of apoptosis of SKOV3 cells seen when treated with compound C2 at 4X, 10X and 40X respectively during AO/PI staining. (D) Cell shape reduced to round due to cell shrinkage and chromatin condensation (green arrow) as a sign of Apoptosis with the appearance of bright yellow nucleus and orange cytoplasm. (E) Membrane blebbing (blue arrows) in the orange fluorescent cells and apoptotic body formation (yellow arrows) in some cells while in others bright green cells with orange nucleus indicating early apoptosis. (F) Membrane blebbing (blue arrows) and apoptotic body formation (yellow arrows). (G) Intact Nucleus of A549 cells untreated (red arrow). (H) Nuclear Fragmentation with compound C2 (green arrows).

2.6 Colony Formation Assay

The long-term antiproliferative effects of the Co(II) complexes were evaluated using a clonogenic assay, which measures the colony-forming ability of cancer cells. Untreated and DMSO-treated cells formed large, dense colonies, confirming their inherent clonogenic potential (Figure 6). Among the tested compounds, C2 showed the strongest inhibition of colony formation in A549, HepG2, and SK-OV-3 cells, while having minimal effect on the colony-forming ability of normal Vero cells, indicating high cancer-cell selectivity (Figure 6).

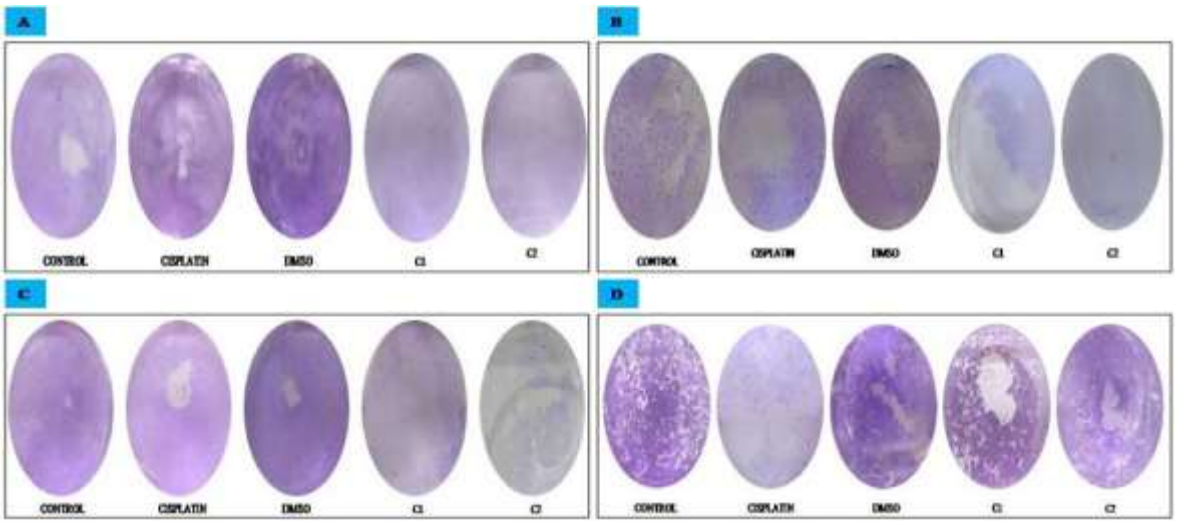

Figure 6. Colony formation assay to assess the impact of C1-C8, Cisplatin, and DMSO (negative control) on the Clonogenic potential of (A) A549, (B) HepG2, (C) SKOV-3, and (D) Vero cells.

2.7 Effect of compounds on induction of apoptosis on cancer cells by DNA Fragmentation Assay

DNA fragmentation, a hallmark of apoptosis, was assessed by agarose gel electrophoresis to confirm the mode

of cell death induced by the Co(II) complexes. Both C1 and C2 produced characteristic DNA laddering in A549, HepG2, and SK-OV-3 cells, confirming apoptosis, whereas untreated controls showed intact DNA (Figure 7A, 7B, 7C). C2 generated the most distinct laddering pattern, indicating stronger pro-apoptotic activity than C1 and cisplatin, consistent with the fluorescence microscopy and clonogenic assay results. In contrast, C2-treated Vero cells exhibited intact high-molecular-weight DNA comparable to untreated controls, indicating negligible toxicity, while C1 caused weak DNA fragmentation and cisplatin induced marked DNA damage(Figure 7D). These findings demonstrate that C2 selectively induces apoptosis in cancer cells while sparing normal cells, supporting its selection for subsequent in vivo studies.

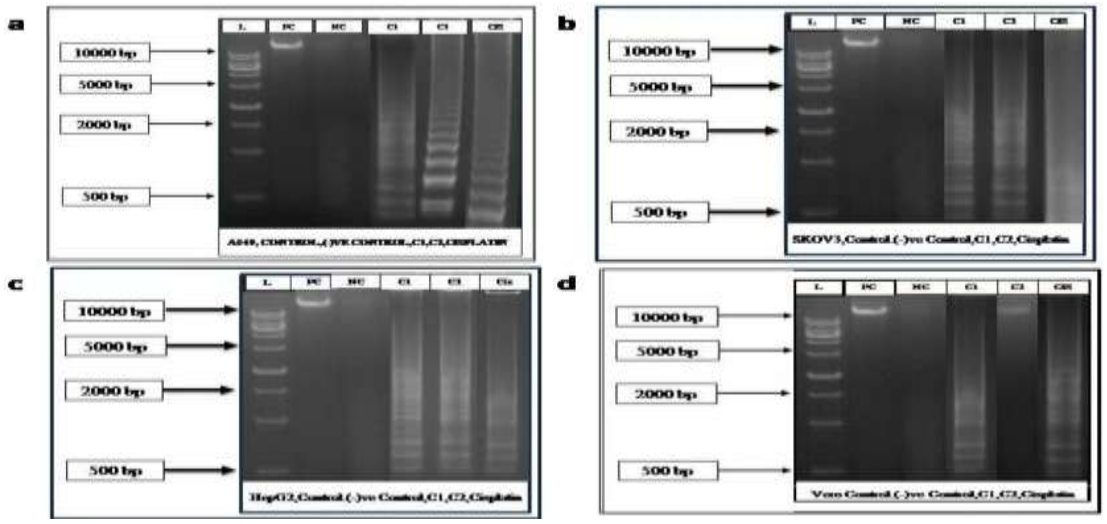

Figure 7. The gel images showing the DNA fragmentation in (a) A549, (b) SKOV-3, (c) HepG2 and (d) Vero cells. L, PC, NC,C1,C2, and CIS, represent the ladder, positive control, negative control, complex C1, complex C2, and cisplatin respectively.

2.8 Cell Cycle Analysis

To elucidate the antiproliferative mechanism of C2, cell cycle analysis was performed by flow cytometry after 24 h of treatment at the respective IC_{50} concentrations. C2 induced significant S-phase arrest in A549, HepG2, and SK-OV-3 cells, accompanied by a reduction in the G2/M population, while the G1 phase remained largely unchanged, indicating inhibition of cancer cell proliferation through S-phase arrest (Figures 8.1–8.3). In contrast, non-cancerous Vero cells exhibited minimal changes in cell cycle distribution for C2, demonstrating the selective action of C2 toward malignant cells (Figure 8.4) unlike Cisplatin which caused G1-phase accumulation, implying a distinct mechanism of cell cycle inhibition.

Figure 8.1. Cell Cycle Analysis and Percentage of cel

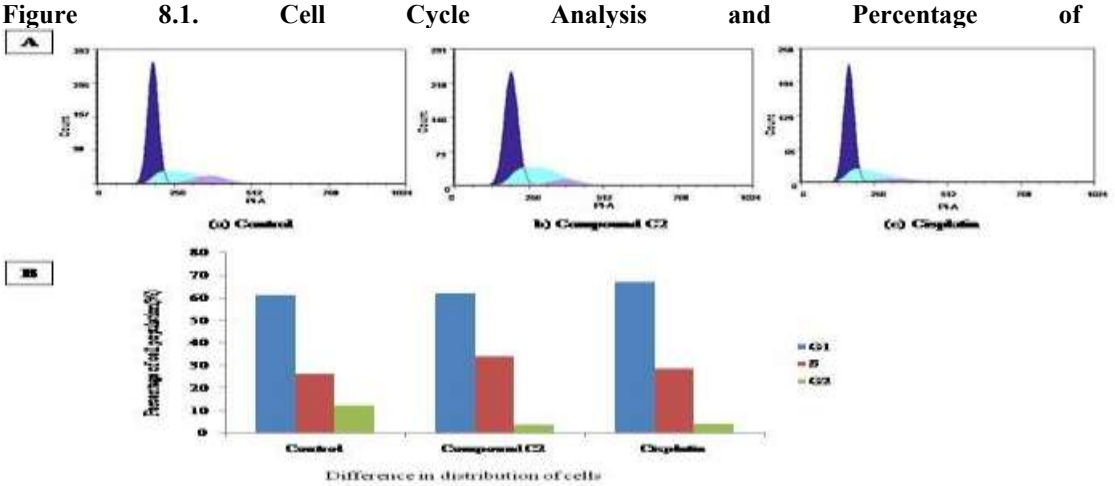

Time	Cycle	(a) Control (%)	(b) Compound C2 (%)	(c) Cisplatin (%)
24 hrs	G1	61.24 ±1.14	62.23 ± 0.62	67.12 ±2.52
	S	26.49 ±0.64	34.15± 2.7	28.70 ±1.72
	G2	12.5 ±1.05	3.70±2.6	4.08 ± 3.04

l

population proliferation of A549 cell line for compound C2. (A) Cell cycle phase distribution of (a) Control (untreated), (b) Compound C2 (1µM), and (c) Cisplatin (1µM) for 24 hours by FACS. (B) Bar graphs represent the percentage changes of cells at the G1, S, and G2 phases for untreated cells, compound C2 and cisplatin. (C) Quantifying the relative proportions of cells in each cell cycle phase.

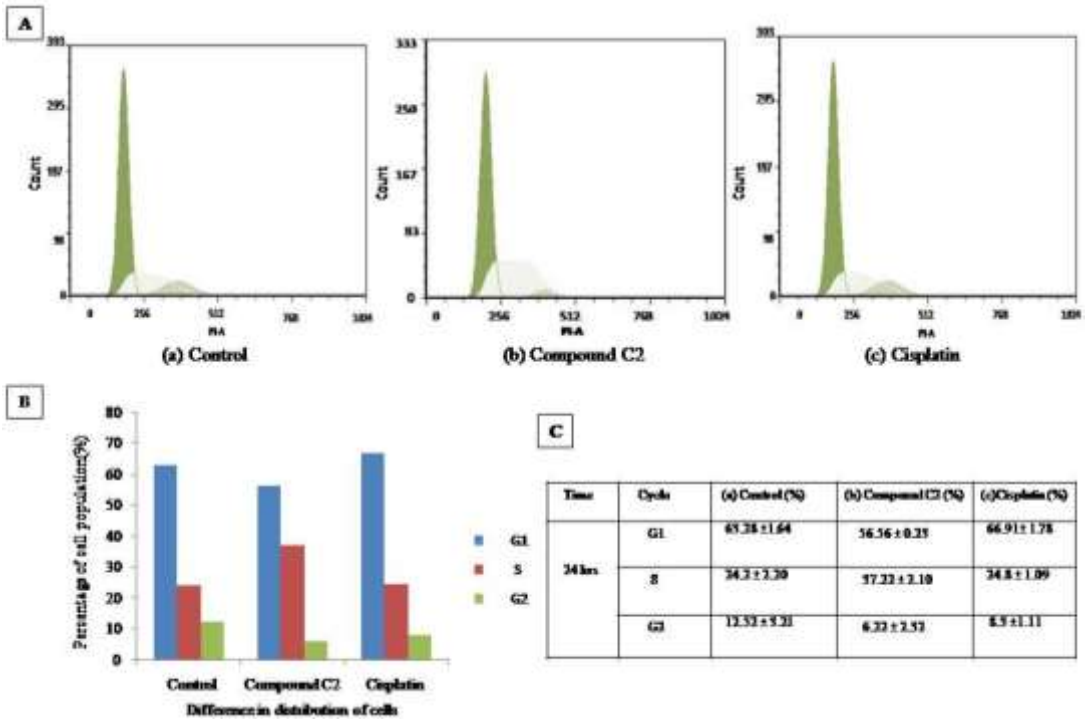

Figure 8.2. Cell Cycle Analysis and Percentage of cell population proliferation of HepG2 cell line for compound C2. (A) Cell cycle phase distribution of (a) Control (untreated), (b) Compound C2 (1µM), and (c) Cisplatin (1µM) for 24 hours by FACS. (B) Bar graphs represent the percentage changes of cells at the G1, S, and G2 phases for untreated cells, compound C2 and cisplatin. (C) Quantifying the relative proportions of cells in each cell cycle phase.

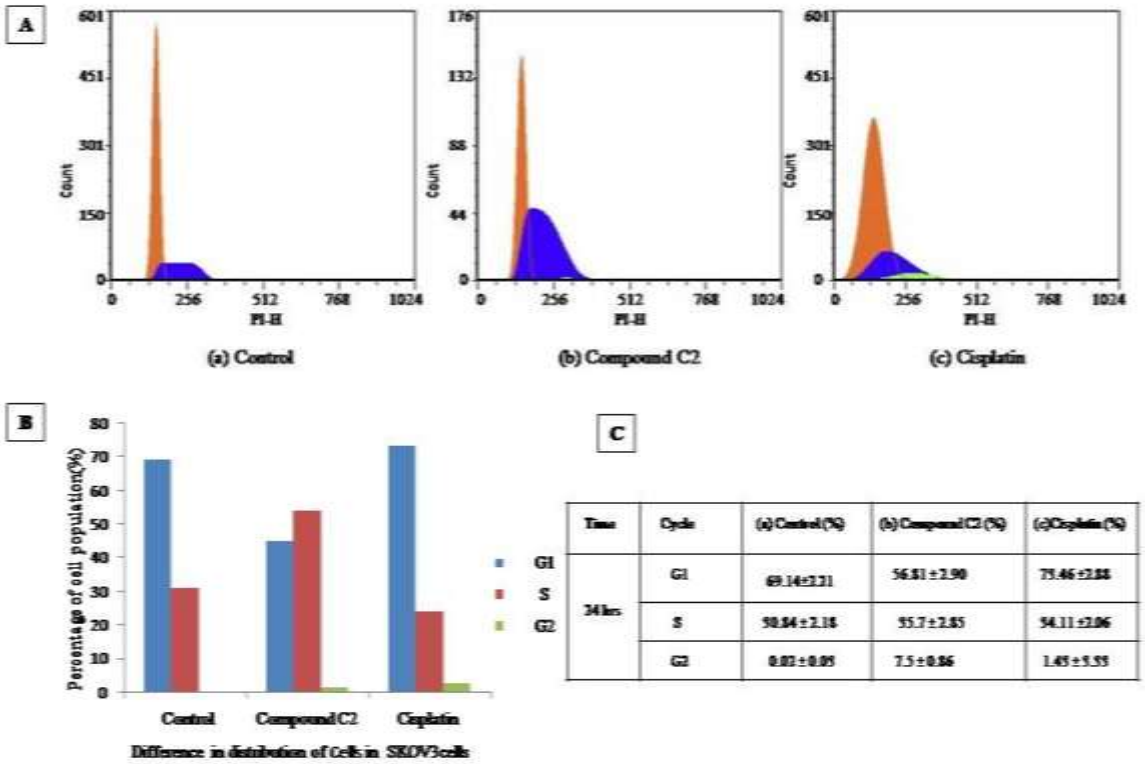

Figure 8.3. Cell Cycle Analysis and Percentage of cell population proliferation of SKOV3 cell line for compound C2. (A) Cell cycle phase distribution of (a) Control (untreated), (b) Compound C2 (1µM), and (c) Cisplatin (1µM) for 24 hours by FACS. (B) Bar graphs represent the percentage changes of cells at the G1, S, and G2 phases for untreated cells, compound C2 and cisplatin. C) Quantifying the relative proportions of cells in each cell cycle phase.

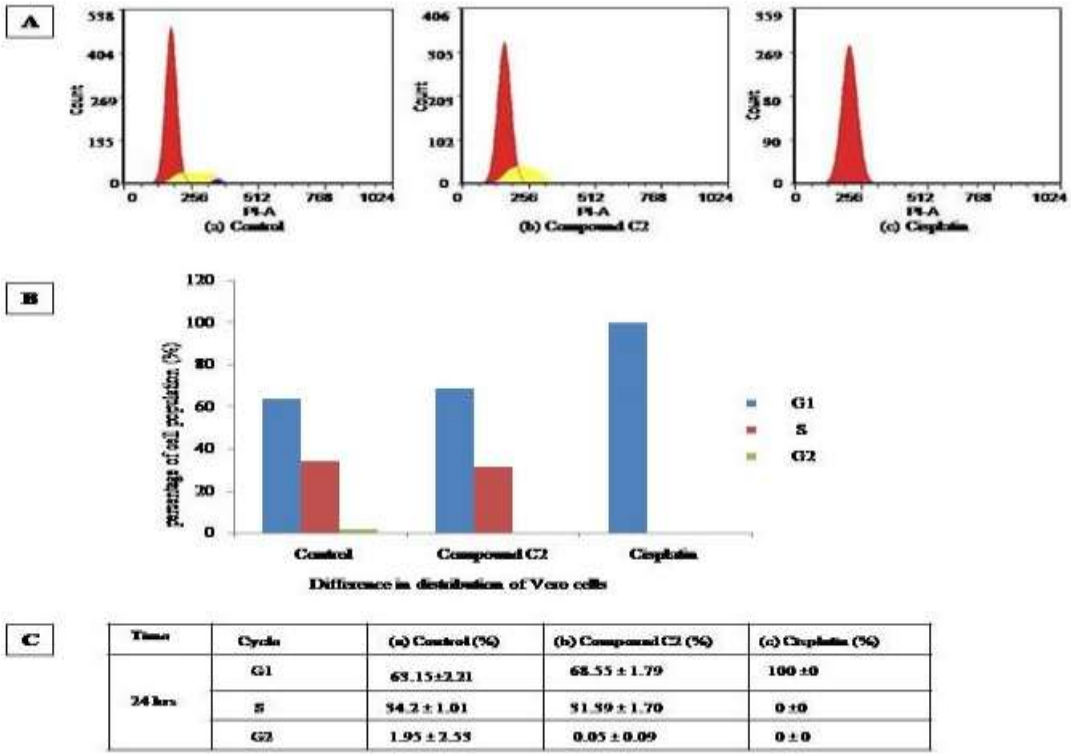

C

Time	Cycle	(a) Control (%)	(b) Compound C2 (%)	(c) Cisplatin (%)
24 hrs	G1	69.15±2.21	68.55 ± 1.79	100 ±0
	S	34.2 ± 1.01	31.59 ± 1.70	0 ±0
	G2	1.95 ± 2.55	0.05 ± 0.09	0 ± 0

Fig 8.4. Cell Cycle Analysis and Percentage of cell population proliferation of Vero cell line for compound C2. (A) Cell cycle phase distribution of (a) Control (untreated), (b) Compound C2 (1µM), and (B) Cisplatin (1µM) for 24 hours by FACS. (B) Bar graphs represent the percentage changes of cells at the G1, S, and G2 phases for untreated cells, compound C2 and cisplatin. (C) Quantifying the relative proportions of cells in each cell cycle phase.

2.9 Results of In Vivo Toxicity

To evaluate its clinical potential, the safety profile of compound C2 was investigated in female Swiss albino mice through acute and subacute toxicity studies, followed by histopathological and immunohistochemical analyses.

2.9.1 Acute Toxicity

Acute toxicity of C2 was evaluated in female Swiss albino mice following OECD Guideline 423. Mortality was observed at 110 mg/kg (1/3 mice), while 130 mg/kg was identified as the LD_{100}. The LD_{50}, calculated using Karber's method, was 121.67 mg/kg. Based on this value, three doses—12.17, 8.11, and 6.08 mg/kg (1/10th, 1/15th, and 1/20th of the LD_{50}, respectively)—were selected for the subsequent subacute toxicity study.

2.9.2 Sub-acute toxicity study based on modulating hematological and biochemical index

A 28-day sub acute toxicity study was conducted in female Swiss albino mice to evaluate the safety of C2. Hematological analysis (Table 2) revealed no significant alterations in RBC, WBC, platelet, or hemoglobin levels at the lowest dose (6.08 mg/kg; 1/20th LD_{50}) compared with controls, while only marginal changes were observed at the medium and high doses. These findings indicate that C2 exhibits minimal hematological toxicity and a more favorable safety profile than conventional platinum-based complexes.

Table 2. Effect of C2 with different doses on hematological parameters of normal female Swiss albino mice

Groups	RBC (/µL)	WBC(/µL)	PLT (×103/µL)	HGB(g/DL)
Control	4.48×106(±0.12)	14.8×103(±0.5)	309×103± 1.64	9.3 (±0.5)
Low dose	4.39×106(±0.20)	14.3×103(±0.3)	310×103±19	8.5(±0.65)
Medium dose	4.58×106(±0.20)	15.8×103(±0.8)	316×103±8	8.7(±0.4)
High dose	5.05×106(±0.5)	17.2×103(±0.2)	326×103±12	9.0(±0.2)

The data were presented as mean±SD of six independent samples from each group. After 28 days of Successive therapy with increasing doses of 1, there has been no significant difference in the Modulation of hematological parameters($p>0.5$).

2.9.3 Biochemical Analysis

Biochemical analysis showed no significant changes in liver function markers (SGOT, SGPT, bilirubin) or kidney function markers (urea and creatinine) following 28 days of C2 treatment at any dose (Table 3; Figures 9 and 10). Consistently, no mortality or treatment-related toxic signs were observed, indicating the absence of significant hepatotoxicity or nephrotoxicity.

2.9.4 Effect of Complex C2 on Liver and kidney Function Tests

C2 caused only mild, dose-dependent changes in liver function markers (SGOT, SGPT, and bilirubin), all of which remained within the normal physiological range. A slight elevation in SGPT and creatinine was observed at the highest dose, suggesting minimal liver and kidney stress without significant hepatotoxicity or nephrotoxicity [Figure 9(A-C) & Figure 10(A,B)]. Overall, C2 did not produce clinically relevant biochemical alterations at either the low (6.08 mg/kg) or high (24.22 mg/kg) dose, indicating that both doses are suitable for subsequent in vivo anticancer studies.

The data were presented as mean±SD of six independent samples from each group. After 28 days of Successive therapy with increasing doses of C2, there has been no significant difference in the Modulation of hematological parameters($p>0.5$).

Table 3. Effect of C2 with different doses on biochemical parameters of normal female Swiss albino mice

Groups	SGOT(U/L)	SGPT(U/L)	Bilirubin(mg/dL)	Urea(/U/L)	Creatinine(mg/DL)
Control	54.76(±.85)	39.88(±1.92)	.5087(±0.01)	18.45(±0.65)	0.33(±0.02)
Low dose	57.30±1.32	42.57(±2.29)	.5254(±0.02)	19.39(±1.86)	0.35(±0.01)
Medium dose	60.94±0.92	44(±5)	.5540(±0.01)	20(±7)	0.37(±0.08)
High dose	62.66±1.05	46(±6)	.5917(±0.0)	23(±3)	0.39(±0.06)

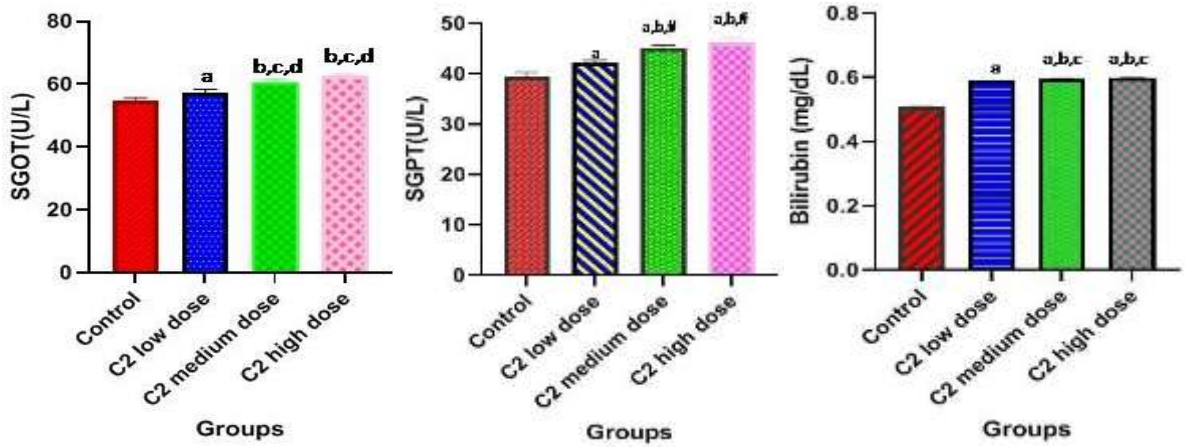

(A) B) (C)

Figure 9. Results of toxicity study of compounds C2 on SGOT, SGPT and Bilirubin levels in female Swiss Albino Mice.

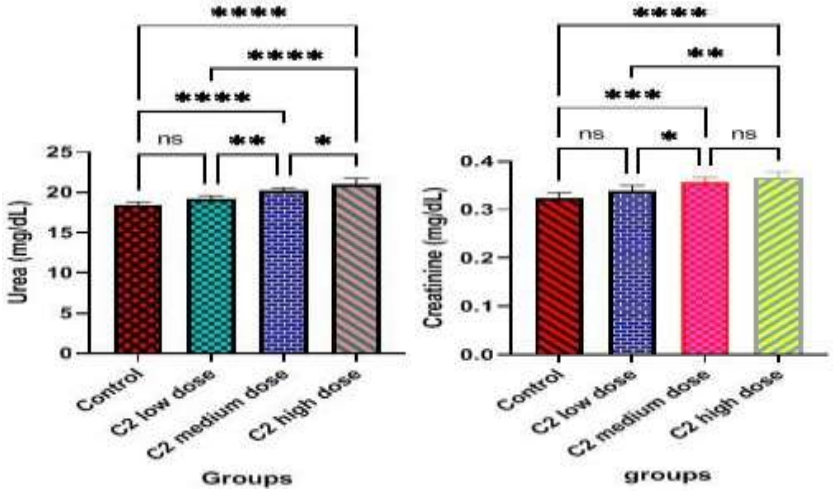

(A) (B)

Figure 10. Results of toxicity study of compounds C2 on Urea and Creatinine levels in female Swiss Albino Mice.

2.9.5 Histopathological evaluation of C2 in Liver

Histopathological examination of liver sections after 28 days of C2 treatment showed dose-dependent but mild changes (Figures 11 and 12). Untreated mice exhibited normal hepatic architecture with well-organized hepatocytes, sinusoids, and central veins. The low dose (1/20th LD_{50}) preserved normal liver morphology, while the medium dose (1/10th LD_{50}) showed mild sinusoidal dilation and early cellular detachment. At the high dose, moderate hepatic alterations, including cytoplasmic vacuolation, sinusoidal dilation, and mild inflammatory cell infiltration, were observed, indicating only mild liver injury.

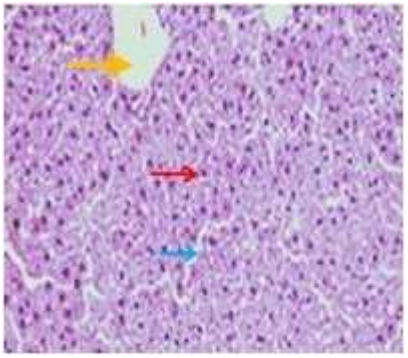

Fig 11: Histopathological section of liver in control mice treated with DMSO with normal hepatocyte (Red arrow), central vein (orange arrow) and blood sinusoids (blue arrow).

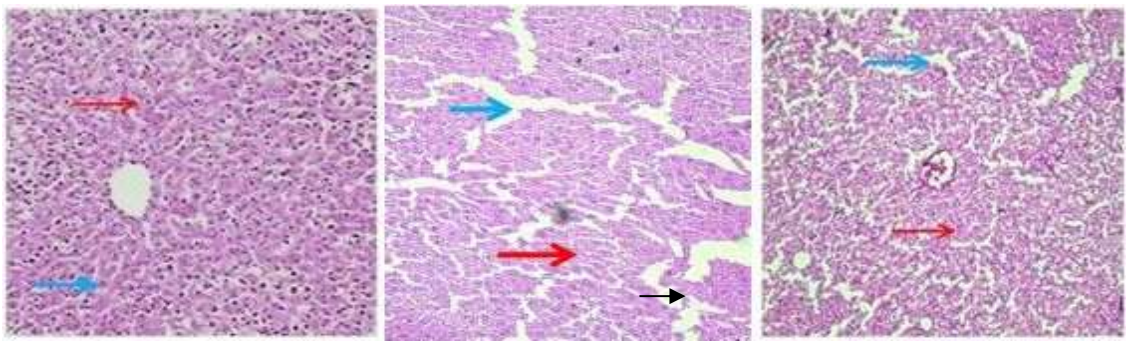

(A) 6.08mg/kg (B) 12.167 mg/kg (C) 24.33 mg/kg

Figure 12. Histopathological section of liver tissue from Swiss albino mice treated with different doses of C2 obtained on 28th day for the sub acute toxicity. Red arrow indicates hepatocyte, blue arrow blood sinusoids and yellow arrow infiltration of blood tissue.

2.9.6 Kidney

Histopathological examination of kidney sections (Figures 13 and 14) revealed normal renal architecture in control mice, including intact glomeruli and renal tubules. C2-treated groups showed no significant renal damage at the low dose and only minimal histological changes at higher doses, consistent with the normal serum urea and creatinine levels. The concordance of hematological, biochemical, and histopathological findings indicates that C2 has a favorable renal safety profile, supporting the selection of both the low (6.08 mg/kg; 1/20th LD_{50}) and high (24.33 mg/kg; 1/5th LD_{50}) doses for subsequent in vivo anticancer studies.

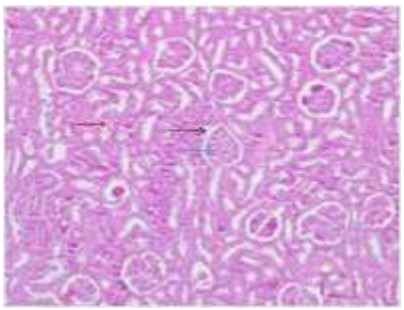

Fig 13: Histopathological section of kidney in control mice treated with DMSO with normal glomeruli (blue arrow), Bowman's capsule (black arrow), and tubules (red arrow).

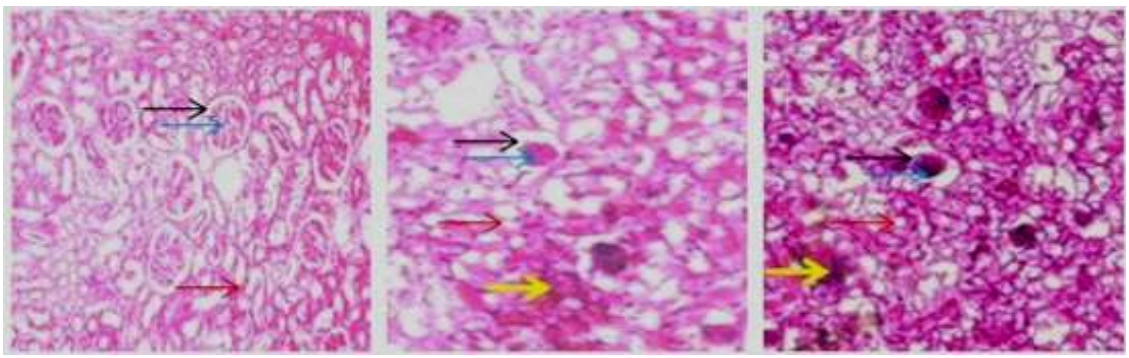

(A) 6.08mg/kg (B) 12.167 mg/kg (C) 24.33 mg/kg

Figure 14. Histopathological section of kidney tissue from Swiss albino mice treated with different doses of C2 obtained on 28th day for the sub acute toxicity.

3. Materials and methods

3.1.Materials

All chemicals and solvents were of analytical grade and obtained from commercial suppliers, including TCI Chemicals, HiMedia (India), and Sigma-Aldrich (USA). Solvents were purified by standard procedures before use unless otherwise stated. The Co(II) β-diketonate complexes, $Co(phen)_2(acac)_2$ (C1) and $Co(dpq)_2(acac)_2$ (C2), were synthesized by the research group led by Dr. Akhtar Hussain, Department of Chemistry, Handique Girls' College, Guwahati, India. Benzo[a]pyrene was purchased from Sigma-Aldrich, and all buffers were prepared using deionized double-distilled water. Hematological and biochemical analyses were performed using automated diagnostic instruments at the Veterinary Clinical Complex and the Department of Veterinary Pathology, College of Veterinary Science, Assam Agricultural University, Guwahati.

3.2 Methods

CHN elemental analysis was performed using a Thermo Finnigan Flash EA 1112 analyzer. Flow cytometric analysis was carried out using a FACS Calibur cell analyzer (Becton Dickinson) at the FL1 channel (595 nm). All solvents were purified before use using the standard purificati method [41].Hematological and biochemical analyses were conducted using automated diagnostic instruments at the Veterinary Clinical Complex and Department of Veterinary Pathology, College of Veterinary Science, Assam Agricultural University, Guwahati.

3.2.1 Synthesis and characterization of C1 and C2

Synthesis and characterization of [Co(phen)2Cl2]Cl](C1)

Complex C1, $Co(phen)_2(acac)_2$, was synthesized by reacting cis-$[Co(phen)_2Cl_2]Cl$ with deprotonated acetylacetone (Hacac) in methanol using triethylamine as a base. The reaction mixture was stirred for 3 h at room temperature, followed by precipitation with $NaClO_4 \cdot H_2O$. The obtained reddish-brown solid was filtered, washed, and vacuum-dried to yield pure C1 (66%). Elemental analysis: calculated C, 56.37; H, 3.75; N, 9.07%; found C, 56.52; H, 3.77; N, 9.09%.

Synthesis and characterization of [Co(dpq)2(acac)](ClO4)2](C2)

Complex C2 was synthesized following a procedure similar to C1 by reacting cis-$[Co(dpq)_2Cl_2]Cl$ with deprotonated diphenylacetylacetone (Ph_2acac) in methanol using triethylamine. The reaction yielded pure $Co(dpq)_2(Ph_2acac)_2$ (C2) after precipitation and purification, with a yield of 71%. Elemental analysis: calculated C, 54.90; H, 3.21; N, 15.52%; found C, 55.12; H, 3.20; N, 15.55%.

3.2.2 Cell culture

Human cancer cell lines A549, SKOV-3, HepG2, and normal Vero cells were obtained from NCCS, Pune, India. Cells were maintained as adherent monolayer cultures in DMEM supplemented with 10% heat-inactivated FBS and 1% penicillin–streptomycin under standard conditions (37°C, 5% CO_2, and 95% air).

3.2.3 Cell Proliferation Assay (MTT Assay)

The antiproliferative activity of cobalt complexes C1 and C2 against A549, HepG2, SK-OV-3, and Vero cells was assessed using the MTT assay [42]. Cells (1×10^5 cells/well) were seeded in 96-well plates, treated with different concentrations of the complexes for 24 and 48 h, and untreated cells served as controls. After treatment, MTT solution (0.5 mg/mL) was added and incubated for 3 h, followed by dissolution of formazan crystals with DMSO. Absorbance was measured at 570 nm using a microplate reader. Cell viability was calculated relative to control cells, and IC_{50} values were obtained from dose–response curves. All experiments were performed in triplicate.

The equation applied for Cell viability calculation: Cell Viability (%) = (Absorbance of treated cells / Absorbance of control cells) × 100.

3.2.4 Morphology change

Morphological changes induced by the test compounds were evaluated using an inverted microscope [43]. Cells (1×10^4 cells/well) were seeded in 96-well plates, incubated for 24 h, and treated with test compounds (10 µg/mL) or cisplatin for an additional 24 h. Untreated cells served as controls. After treatment, cells were washed with PBS, and morphological alterations were examined and imaged using an inverted microscope (Lawrence and Mayo Lynx LM-52-3501).

3.2.5 Crystal Violet Staining

Cell morphology following treatment with the test compounds and cisplatin was evaluated by crystal violet staining [39]. Cells (5×10^4) were seeded in culture plates, incubated for 24 h, and treated with compounds or cisplatin (10 µg/mL) for an additional 24 h. Untreated cells served as negative controls. After treatment, cells were fixed with 0.4% paraformaldehyde, stained with crystal violet, and morphological changes were examined using an inverted microscope (Lawrence and Mayo Lynx LM-52-3501).

3.2.6 AO/PI Double Staining Assay

Cell viability and apoptosis were evaluated by acridine orange/propidium iodide (AO/PI) dual fluorescence staining [40]. A549, HepG2, SK-OV-3, and Vero cells (2×10^5 cells/dish) were treated with the test compounds at their IC_{50} concentrations for 24 h, followed by PBS washing and AO/PI staining. After 45 min incubation, cells were examined using a Leica fluorescence microscope. Viable cells showed green fluorescence (AO), whereas non-viable cells exhibited orange fluorescence (AO+PI) and necrotic cells exhibited red fluorescence (PI).

3.2.7 Colony Formation Assay

The clonogenic potential of A549, HepG2, SK-OV-3, and Vero cells was assessed by colony formation assay [44]. Cells (1×10^3 cells/well) were seeded in 6-well plates, treated with the test compounds for 24 h, and allowed to grow for 15 days in fresh medium. Formed colonies were fixed with 70% ethanol, stained with 0.01% crystal

violet, and analyzed after PBS washing.

3.2.8 DNA Fragmentation Assay for Apoptosis:

DNA fragmentation was assessed as an apoptotic marker Cells (5×10^6 cells/mL) were treated with the test compounds for 24 and 48 h, followed by harvesting and genomic DNA extraction using the Wizard® Genomic DNA Purification Kit. Extracted DNA was analyzed by agarose gel electrophoresis to evaluate apoptotic DNA fragmentation patterns [41].

3.2.9 Cell Cycle Analysis

Cell cycle distribution was analyzed by flow cytometry [45]. A549, HepG2, SK-OV-3, and Vero cells (5×10^5 cells/dish) were treated with the test compounds for 24 h, fixed with 70% ethanol, and stained with RNase A/propidium iodide. DNA content was analyzed using a FACS Calibur flow cytometer (BD Biosciences), and cell cycle profiles were generated using FCS Express software. Experiments were performed in triplicate.

3.3 In vivo study

3.3.1 Maintenance of Animals:

Healthy female Swiss albino mice (6–8 weeks old) were obtained from the Animal House, Department of Zoology, Gauhati University, Assam, India. Animals were maintained under controlled temperature, humidity, and 12 h light/dark cycle conditions with free access to standard pellet diet and water. Mice were acclimatized for 7 days before experimentation and randomly assigned to experimental groups. All procedures were conducted following Institutional Animal Ethical Committee approval (IAEC/2024/Ethical-Per/PhD-IAEC/2024-1).

3.3.2 Acute dose toxicity study:

Acute toxicity of C2 was evaluated according to OECD Guideline 423 (Acute Toxic Class Method) [46]. Female Swiss albino mice were administered C2 at doses of 100, 110, 120, and 130 mg/kg body weight after 3–4 h fasting. Animals were monitored for behavioral changes, toxic signs, and mortality for 72 h. The LD_{50} value was calculated, and appropriate doses with minimal toxicity were selected for subsequent in vivo studies [46].

3.3.3. Sub acute toxicity study:

Subacute toxicity of C2 was evaluated according to OECD Guideline 407 for 28 days [47]. Female Swiss albino mice were administered C2 at 1/10th, 1/15th, and 1/20th of the LD_{50} doses, while the control group received DMSO only. Animals were monitored daily for behavioral changes, body weight, food and water intake, fecal condition, and body temperature.

3.3.4 Hematology and Biochemical analysis:

On day 29, mice were fasted for 4 h, anesthetized, and blood samples were collected via retro-orbital puncture before euthanasia. Serum was separated by centrifugation and analyzed for biochemical markers (urea, creatinine, SGOT, and SGPT) using an automated clinical chemistry analyzer [48]. Hematological parameters (RBC, WBC, HGB, and PLT) were evaluated from heparinized blood using an automated hematology analyzer [49]. Results from all dose groups were compared to determine the optimal dose with minimal toxicity for subsequent in vivo anticancer studies.

3.3.5 Histopathological analysis

Liver and kidney tissues from all experimental groups were fixed in 10% neutral buffered formalin, paraffin-embedded, sectioned (4 μm), and stained with hematoxylin and eosin (H&E), reticulin, and PAS following standard protocols [50]. The stained sections were examined and photographed using a bright-field microscope.

4. Statistical Analysis

All in vitro experiments were performed in triplicate, and data were expressed as mean ± SD. IC_{50} values were calculated by nonlinear regression analysis using Graph Pad Prism 9 software. Statistical significance between treated and control groups was evaluated using the t-test, with $p < 0.05$ considered significant. In vivo data ($n = 6$/group) were expressed as mean ± SD and analyzed using one-way ANOVA followed by Tukey's post hoc test in Graph Pad Prism 9 software. Significance levels were set at $p < 0.05$, 0.01, 0.001, and 0.0001.

5. Conclusions

In summary, this study demonstrates the potential anticancer activity of β-diketonate-derived cobalt complexes. The complexes effectively inhibited cancer cell proliferation through apoptosis induction, with C2 showing high selectivity and minimal toxicity toward normal cells compared with cisplatin. Cell migration and multiple live/dead assays further supported their anticancer efficacy. In vivo acute and subacute toxicity studies of C2 in female Swiss albino mice revealed minimal hematological, biochemical, and histopathological alterations, indicating a favorable preliminary safety profile. However, further comprehensive in vivo investigations are required to confirm its therapeutic potential and clinical applicability.

Acknowledgements

We are thankful to Department of Zoology for giving permission to carry out the in vivo experiments in their animal house and providing the animals. We are thankful Dr. Abhijit Deka, Veterinary Clinical Complex (VCC), Department of Pathology, and Dr Dip Saikia, Department of Biotechnology, Veterinary College, AAU Khanapara, Guwahati, Assam for the analysis of *in vivo* study. We are also thankful to Dr. Ranadeep Gogoi and Maihur Basumatary of Molecular Oncology Laboratory, State Cancer Institute, Guwahati, Assam for helping in the *in vitro* study.

Conflicts of Interest

The authors declare no conflicts of interest.

References

1. World Health Organization (WHO). Cancer Fact Sheet. Updated 2025. https://www.who.int/news-room/fact-sheets/detail/cancer
2. Bray F, Laversanne M, Sung H, Sung H., Ferlay J., Siegel R.L., Soerjomataram I., Jemal A., Global cancer statistics 2024: GLOBOCAN estimates of incidence and mortality worldwide for 36 cancers in 185 countries. CA: A Cancer Journal for Clinicians. 2024;74(3):229–263. https://doi.org/10.3322/caac.21834.
3. S. Pilleron, E. Soto-Perez-de-Celis, J. Vignat, J. Ferlay, I. Soerjomataram, F. Bray, D. Sarfati, Int.J.Cancer 148(2021) 601-608.https://doi.org/10.1002/ijc.33232
4. Kamal, A.; Kumar, G.B.; Nayak, V.L.; Reddy, V.S.; Shaik, A.B.; Reddy, M.K. Design, synthesis and biological evaluation of imidazopyridine/imidazopyrimidine-benzimidazole conjugates as potential anticancer agents. Med. Chem. Commun. 2015, 6, 606–612.
5. Yang, L.L.; Lee, C.Y.; Yen, K.Y. Induction of apoptosis by hydrolyzable tannins from Eugenia jambos L. on human leukemia cells. Cancer Lett. 2000, 157, 65–75.
6. D. L. Ma, H. Z. He, K. H. Leung, D. S. H. Chan, C. H.Leung, Angew. 52 (2013) 7666-7682.https://doi.org/10.1002/anie.201208414
7. P. Jia, R. Ouyang,P. Cao, X. Tong, X. Zhou, T. Lei, S. Zhou, J.Coord Chem. 70 (2017) 2175-2201.https://doi.org/10.1080/00958972.2017.1349313
8. B. Rosenberg, L. Van Camp, T. Krigas, Nature. 205 (1965) 698–699.https://doi.org/10.1038/205698a0. 818
9. C. Rancoule, J.-B. Guy, A. Vallard, M. Ben Mrad, A. Rehailia, N. Magné, Les 50 ans du cisplatine, Bull. Cancer (Paris). 104 (2017) 167–176. https://doi.org/10.1016/j.bulcan.2016.11.011. 821
10. S. Dilruba, G.V. Kalayda, Cance Chemother. Pharmacol. 77 (2016) 1103–1124. https://doi.org/10.1007/s00280-016-2976-z. 823
11. D. Elias, B. Raynard, M. Bonnay, M. Pocard, Eur. J. Surg. Oncol. EJSO. 32 (2006) 607–613
12. https://doi.org/10.1016/j.ejso.2006.03.004
13. Bera A., Sarkar T., Upadhay A., Hussain A., Coord. Chem. Rev.2025, 541, 216847. https://doi.org/10.1016/j.ccr.2025.216847
14. Bauer JA, Lupica JA, Schmidt H, Morrison BH, Haney RM, Masci RK, Lee RM, Didonato JA, Lindner DJ. Nitrosylcobalamin potentiates the anti-neoplastic effects of chemotherapeutic agents via suppression of survival signaling. PLoS One. 2007; 2:e1313. [PubMed: 18074035]
15. Gupta Y, Kohli DV, Jain SK. Vitamin B12-mediated transport: a potential tool for tumor targeting of antineoplastic drugs and imaging agents. Crit Rev Ther Drug Carrier Syst. 2008; 25:347–379. [PubMed: 18540842]
16. Ruiz-Sanchez P, Konig C, Ferrari S, Alberto R. Vitamin B(12) as a carrier for targeted platinum delivery: in vitro cytotoxicity and mechanistic studies. J Biol Inorg Chem. 2011; 16:33–44. [PubMed: 20803225]
17. Munteanua C.R., Suntharalingam K., Dalton Trans.2015, 44, 13796–13808. https://doi.org/10.1039/C5DT02101D
18. Maghool, F.; Emami, M.H.; Alipour, R.; Mohammadzadeh, S.; Sereshki, N.; Dehkordi, S.A.E.; Fahim, A.; Tayarani-Najaran, Z.; Sheikh, A.; Kesharwani, P.; et. al. J. Trace Elem. Med. Biol. 2023, 78, 127153.
19. Meza-Morales, W.; Alvarez-Ricardo, Y.; Obregón-Mendoza, M.A.; Arenaza-Corona, A.; Ramírez-Apan, M.T.; Toscano, R.A.; Poveda-Jaramillo, J.C.; Enríquez, R.G. RSC Adv. 2023, 13, 8577–8585.
20. Zhou, S.; Li, J.B.; Yu, J.; Wang, Y.Q.; Liu, H.Z.; Lin, G.M.; He, Z.G.; Wang, Y.J. Mater. Sci. Eng. C 2021, 121, 111835.
21. Qin, Q.P.; Wei, Z.Z.; Wang, Z.F.; Huang, X.L.; Tan, M.X.; Zou, H.H.; Liang, H. Chem. Commun. 2020, 56, 3999–4002.
22. Wu, R.H.; Mei, X.T.; Ye, Y.B.; Xue, T.; Wang, J.S.; Sun, W.J.; Lin, C.X.; Xue, R.X.; Zhang, J.B.; Xu, D.H. Pharmacol. Res. 2019, 150, 104454–104463.
23. Greish, K.; Pittala, V.; Taurin, S.; Taha, S.; Bahman, F.; Mathur, A.; Jasim, A.; Mohammed, F.; El-Deeb, I.M.; Fredericks, S.; et. al. 2018, 8, 884.
24. Banerjee, S.; Chakravarty, A.R. Acc. Chem. Res. 2015, 48, 2075–2083.
25. Goswami, T.K.; Gadadhar, S.; Gole, B.; Karande, A.A.; Chakravarty, A.R. Eur. J. Med. Chem. 2013, 63, 800–810.
26. Vajragupta, O.; Boonchoong, P.; Watanabe, H.; Tohda, M.; Kummasud, N.; Sumanont, Y. Free Radic. Biol. Med. 2003, 35, 1632–1644.
27. Hema, M.K.; Karthik, C.S.; Warad, I.; Lokanath, N.K.; Zarrouk, A.; Kumara, K.; Pampa, K.J.; Mallu, P. J. Mol. Struct. 2018, 1157, 69–77.
28. Pramanik, A.; Laha, D.; Pramanik, P.; Karmakar, P. Drug Target. 2014, 22, 23–33.
29. Xu, D.F.; Shen, Z.H.; Shi, Y.; He, Q.; Xia, Q.C. Russ. J. Coord. Chem. 2010, 36, 458–462.
30. T. Mosmann, “Rapid Colorimetric Assay for Cellular Growth and Survival: Application to Proliferation and Cytotoxicity Assays,” Journal of Immunological Methods 65 (1983): 55–63, https://doi.org/10.1016/0022-1759(83)90303-4
31. Bahadar H, Abdollahi M. Inappropriate use of the term "cytotoxicity" in scientific literature. Daru 2015;23:5–6. https://doi.org/10.1186/s40199-015-0102-0.
32. C. Zhang, C. Xu, X. Gao, and Q. Yao, “Platinum-Based Drugs for Cancer Therapy and Anti-Tumor Strategies,” Theranostics 12 (2022): 2115–2132.
33. S. Dilruba and G. V. Kalayda, “Platinum-Based Drugs: Past, Present and Future,” Cancer Chemotheraphy and Pharmacology 77 (2016): 1103–1124, https://doi.org/10.1007/s00280-016-2976-z.
34. S. Alassadi, M. J. Pisani, and N. J. Wheate, “A Chemical Perspective on the Clinical Use of Platinum-Based

Anticancer Drugs," Dalton Transactions 51 (2022): 10835–10846, https://doi.org/10.1039/ D2DT01875F.
35. R. Oun, Y. E. Moussa, and N. J. Wheate, "The Side Effects of Platinum-Based Chemotherapy Drugs: A Review for Chemists," Dalton Transactions 47 (2018): 6645–6653, https://doi.org/10.1039/ C8DT00838H.
36. Kotnala S., Tiwari S., Nayak A., et al., "Impact of Heavy Metal Toxicity on the Human Health and Environment," Science of the Total Environment 987 (2025): 179785, https://doi.org/10.1016/j.scitotenv.2025. 179785
37. Lica J. J., Wieczór M., Grabe G. J., Heldt M., Effective Drug Concentration and Selectivity Depends on Fraction of Primitive Cells. Int. J. Mol. Sci. 2021, 22(9), 4931; https://doi.org/10.3390/ijms22094931
38. Zhao F., Zhao H., Wenlong Wu, Weifan Wang and Weilin Li, Research on Anthocyanins from Rubus "Shuofeng" as Potential Antiproliferative and Apoptosis-Inducing Agents. Advance in Biological Activities of Functional Food. Foods 2023, 12(6), 1216. https://doi.org/10.3390/foods12061216
39. L. Sliwka, ´ K. Wiktorska, P. Suchocki, M. Milczarek, S. Mielczarek, K. Lubelska, T. Cierpiał, P. Łyzwa, ˙ P. Kiełbasinski, ´ A. Jaromin, A. Flis, Z. Chilmonczyk, R. Moreno-Sanchez, The comparison of MTT and CVS assays for the assessment of anticancer agent interactions, PLoS One 11 (5) (2016) e0155772. https://wiki.oroboros.at/index.php/Lica_2018_Stem_Cells_Dev
40. M. Feoktistova, P. Geserick, M. Leverkus, Crystal violet assay for determining viability of cultured cells, Cold Spring Harb Protoc 2016 (2016) 343–346, https://doi.org/10.1101/PDB.PROT087379
41. Rani N., Rawat K., Saini M., Yadav S., Syeda S., Saini K., and Shrivastava A. Comparative In Vitro Anticancer Study of Cisplatin Drug with Green Synthesized ZnO Nanoparticles on Cervical Squamous Carcinoma (SiHa) Cell Lines, ACS Omega 2023, 8, 14509−14519 (https://pubs.acs.org/doi/10.1021/acsomega.2c08302).
42. Perrin D. D., Armarego W. L. F., and Perrin D. R., Purification of Laboratory Chemicals (Pergamon Press, 1980).
43. T. Mosmann, "Rapid Colorimetric Assay for Cellular Growth and Survival: Application to Proliferation and Cytotoxicity Assays," Journal of Immunological Methods 65 (1983): 55–63, https://doi.org/10.1016/0022-1759(83)90303-4.
44. Muthukumar V., Vanisree A.J. Molecular interaction of Survivin and Piperine by computational docking analyses for neuroblastoma targeting, Ann Neurosci. 2011 Oct;18(4):145–147. doi: 10.5214/ans.0972.7531.1118404
45. Zhang H., Tian L., Xiao R., Zhou Yi, Zhang Y., Hao J., Liu Y., Wan j., Anticancer effect evaluation in vitro and in vivo of iridium(III) polypyridyl complexes targeting DNA and mitochondria. https://doi.org/10.1016/j.bioorg.2021.105290
46. M. Aswathy, P. Dey, M. Hegde, et al., "Natural Prenylflavones From the Stem Bark of Artocarpus altilis: Promising Anticancer Agents for Oral Squamous Cell Carcinoma Targeting the Akt/mTOR/STAT-3 Signaling Pathway," ACS Omega 9 (2024): 24252–24267, https://doi.org/10.1021/ acsomega.3c08376.
47. Shah, A.H.; Qureshi, S.; Tariq, M.; Ageel, A.M. Toxicity studies on six plants used in the traditional Arab system of medicine. Phytother. Res. 1989, 3, 25–29.
48. Tamta A., Chaudhary M., Sehgal R., A 28-days sub-acute toxicity study in swiss albino mice to evaluate toxicity profile of neurotol plus (mannitol and glycerol combination), Int. J. Biomed. Sci. IJBS. 5 (2009) 428–433.
49. Hussain A , Al Ajmi M.F., Rehman Md.T., Khan A.A., Shaikh P.A. and Khan R.A. Evaluation of Transition Metal Complexes of Benzimidazole-Derived Scaffold as Promising Anticancer Chemotherapeutics. Molecules 2018, 23, 1232. 10.3390/molecules23051232
50. Edwards, C.R.W.; Bouchier, I.A.D. Davidson's Principles and Practice Medicine; Churchill Livingstone Press: London, UK, 1991; p. 492.
51. R.W. Horobin, 9 - Theory of histological staining, in: S.K. Suvarna, C. Layton, J.D. Bancroft (Eds.), Bancrofts Theory Pract. Histol. Tech. Eighth Ed., Elsevier, 2019: pp. 114–125. https://doi.org/10.1016/B978-0-7020-6864-5.00009-8.